NAVAL AIR ENGINEERING CENTER

LAKEHURST. N.J.
08733

APPLICATION OF ULTRASONIC "F-SCAN" TO THE
INSPECTION OF COMPOSITE MATERIALS

Advanced Technology Office
Support Equipment Engineering Department
Naval Air Engineering Center
Lakehurst, New Jersey 08733

15 APRIL 1982

Final Report
AIRTASK A03V3400/051B/1F41461000

DTIC
ELECTE
MAY 3 1982

H

Prepared for

Commander, Naval Air Systems Command
AIR-340E
Washington, DC 20361

82 05 03 009

APPLICATION OF ULTRASONIC "F-SCAN" TO THE
INSPECTION OF COMPOSITE MATERIALS

Prepared by: _Joseph L. Rose_
Joseph L. Rose
Ultrasonic Research Laboratory
Drexel University

Reviewed by: _Peter V. Ciekurs_
Peter V. Ciekurs, P.E.
Advanced Technology Office

Approved by: _F. E. Evans_
F. E. Evans
Support Equipment Engineering Superintendent

4-15-82 NM

REPORT DOCUMENTATION PAGE		READ INSTRUCTIONS BEFORE COMPLETING FORM
1. REPORT NUMBER NAEC-92-159	2. GOVT ACCESSION NO. AD A114-072	3. RECIPIENT'S CATALOG NUMBER
4. TITLE (and Subtitle) APPLICATION OF ULTRASONIC "F-SCAN" TO THE INSPECTION OF COMPOSITE MATERIALS		5. TYPE OF REPORT & PERIOD COVERED FINAL
		6. PERFORMING ORG. REPORT NUMBER
7. AUTHOR(s) JOSEPH L. ROSE J. BRUCE NESTLEROTH SHAHAB NEGAHBAN		8. CONTRACT OR GRANT NUMBER(s) N68335-80-C-1119
9. PERFORMING ORGANIZATION NAME AND ADDRESS ULTRASONICS RESEARCH LAB DREXEL UNIVERSITY PHILADELPHIA, PA 19104		10. PROGRAM ELEMENT, PROJECT, TASK AREA & WORK UNIT NUMBERS AIRTASK A03V3400/051B/1F41461000
11. CONTROLLING OFFICE NAME AND ADDRESS NAVAL AIR SYSTEMS COMMAND WASHINGTON, DC 20361		12. REPORT DATE 15 April 1982
		13. NUMBER OF PAGES 45
14. MONITORING AGENCY NAME & ADDRESS(If different from Controlling Office) NAVAL AIR ENGINEERING CENTER CODE 92A3 LAKEHURST, N.J. 08733		15. SECURITY CLASS. (of this report) UNCLASSIFIED
		15a. DECLASSIFICATION/DOWNGRADING SCHEDULE

16. DISTRIBUTION STATEMENT (of this Report)

APPROVED FOR PUBLIC RELEASE:
DISTRIBUTION UNLIMITED

17. DISTRIBUTION STATEMENT (of the abstract entered in Block 20, if different from Report)

18. SUPPLEMENTARY NOTES

19. KEY WORDS (Continue on reverse side if necessary and identify by block number)

NONDESTRUCTIVE TESTING
ULTRASONICS
COMPOSITE MATERIALS

20. ABSTRACT (Continue on reverse side if necessary and identify by block number)

1. Composites are now being used in high strength, low weight applications such as the aircraft industry. Difficulties arise in the nondestructive testing and evaluation of these materials because of their fibrous nature. The traditional ultrasonic C-scan technique is often found very limiting. A new technique called F-scanning (Feature scanning) has been developed that examines many features (characteristics) of the ultrasonic waveform such as amplitude ratios and frequency shifts. These features can be better used to locate

DD FORM 1473 EDITION OF 1 NOV 65 IS OBSOLETE
1 JAN 73
S/N 0102-LF-014-6601

20. Abstract (cont'd)

defects. This technique was used to evaluate a composite patch that had
severe void content. Photomicrographs were used to determine defective
and non-defect areas for correlation with the results obtained in the F-map
process. These results showed an overall index of performance of 87.5
percent correct decisions.

TABLE OF CONTENTS

Accession For

NTIS GRA&I ☑
DTIC TAB ☐
Unannounced ☐
Justification___

By___
Distribution/
Availability Codes

Dist	Avail and/or Special

DTIC
COPY
INSPECTED
2

1

LIST OF TABLES

LIST OF ILLUSTRATIONS

I. INTRODUCTION

A. Composite materials are being established as a new and exciting engineering material and are now being widely used in various applications. Their success is due to such physical properties as high specific strength and stiffness. Unfortunately, difficulties arise in the detection of damage in the materials that occurs either during the manufacturing process or while in service. Extensive papers have been published in the field of composite damage analysis. A wide range of topics has been examined in the microscopic and macroscopic levels(references (a) through (e)). The need for a fast and efficient nondestructive testing technique to insure the quality of a composite is increasingly rising. The main objective of Nondestructive Test (NDT) is to locate the defect's size, shape, and criticality. Various disciplines of NDT are presently being researched, and several studies have discussed and compared these techniques specifically for composite materials (references (f) through (h)).

B. Ultrasonics is one of the most commonly used techniques of detecting defects in composities. For many years, the popular method based on attenuation of high-frequency ultrasonic waves through the sample, has been the subject of many publications (references (i) through (l)). Most recently, Daniel and Libert (reference (l)) did a study on flaw growth in composite materials by using ultrasonic monitoring techniques of C-scanning and A-scanning. They concluded that better techniques have to be developed for detecting flaws such as porosity, fiber breaks, and matrix crazing. However, in the past decade, several alternatives have been introduced. Such concepts as frequency shift analysis and adaptive learning techniques are evolving as the new tools of Nondestructive Evaluation (NDE) of composite materials (references (m) through (q)). The goal of this project is to develop an ultrasonic scanning technique that can be used to more reliably detect defects in composites. This technique is called "F-scan", which stands for feature scanning. The F-scan process utilizes a computer to extract and store many features, that is characteristics of the ultrasonic signals, and then to use the features to locate defects (reference (r)).

C. The newly developed tool would be used to detect defects in a composite patch used to repair the composite skins of aircraft wings. This report explains the development of the tool and results of a sample problem.

NOTE: References appear on pages 17 and 18.

II. BACKGROUND

A. Many types of defects can be observed in fibrous composite structures. These are induced either during the fabrication processes or as a result of actual in-service conditions, environmental conditions, and aging. The most frequently occurring flaws according to reference (s) are:

1. Porosity or void content - They come about by less than 100% dense material resulting from incomplete flow of the matrix in the bonding process. The void content will significantly affect the composite's properties. Higher void content indicates lower fatigue resistance and less resistance to such environmental conditions as water penetration and weathering.

2. Debonding - The separation of fibers from a matrix in the fiber-rich region of the plies is called debonding.

3. Delaminations - The separation of laminates from each other in a laminated composite.

B. A material may fail when subjected to cycle loading even if the load is less than the ultimate strength of that material (fatigue).

1. Unidirectional fibrous composites have excellent fatigue resistance when loaded in the fiber direction. However, the fibrous composites are generally used in the form of laminates. A laminate consists of several plies which are stacked together, each ply having a different angle orientation. Therefore, the angle between load direction and fiber direction varies from ply to ply. Weaker plies fail at an earlier stage under loading. The initial damage may appear at the early stage of fatigue life, but the propagation rate is much slower in composites than all of the isotropic metals.

2. There are several types of damage that can happen during the fatigue of composites, starting with debonding in which the fibers are perpendicular or at a large angle to the loading direction. The crack is generally perpendicular to the load direction and propagates across the width of the fiber and the ply. The tip of this cross-ply crack produces a stress concentration which in turn causes delamination between the plies. As the number of cycles increases the damage becomes more extensive. At this stage, longitudinal-ply cracks can appear, which do not follow any pattern as in the case of cross-ply cracks.

C. ULTRASONICS

1. Ultrasonics is an NDT technique that uses high-frequency (1-20 MHz) sound waves to locate defects (references (q) and (t)). This energy is sent to the test specimen by a piezoelectric transducer, is reflected by an interface between two materials, and then returns to the transducer. By measuring the arrival time of the echo and the wave speed of the material, the depth of a reflector can be calculated. If the design of the specimen dictates that the

material should be continous at that depth, then the reflection is returning from the discontinuity which must therefore be a defect.

2. This technique works when scanning specimens made from homogeneous materials such as aluminum, steel, plastics, etc.; difficulty arises when examining nonhomogeneous materials such as composites. The fiber and laminar construction of composites give many interfaces from which the ultrasonic energy can reflect. This causes many echoes to occur throughout the specimen which makes it difficult to distinguish the defects from the noise (multiple non-defect echoes). Also the multiple interfaces attenuate most of the sound energy before it penetrates the entire composite which makes it impossible to locate defects in that part of the specimen. Also, the attenuation is more severe with higher frequencies. However, when the size of defects is small, such as in composites, higher resolution is needed to detect these defects, but high resolution is associated with higher frequencies which are attenuated by the composite. This is a difficult problem to overcome and the solution usually calls for a compromise in resolution.

D. C-SCAN AND F-SCAN

1. Composite specimens are usually inspected with an automated system called a C-scan. In the C-scan process, the ultrasonic transducer and the specimen are placed in a water bath that acts as a couplant medium for the ultrasonic wave to travel through. The return echoes are gated to include only echoes from the composite. An amplitude threshold is selected so that if the echo amplitude is above the threshold, it is considered a bad area and below this threshold is considered a good area. The transducer is connected to a mechanical device that moves the transducer over the entire specimen. This device also has a plotting system which marks where the threshold was broken.

2. Difficulties arise in the C-scan process because of the physical constraints imposed by composites that were discussed before. The multiple echoes from the laminates and fibers and the attenuation of signal make it difficult to set a threshold. Because of these difficulties, an enhancement was developed called F-scan (Feature scanning). A feature is characteristic of the ultrasonic waveforms. Examples are: rise time, fall time, and pulse duration of the ultrasonic waveform, as well as characteristics of the frequency spectrum. Thresholds can be set on these features similarly to those set in the C-scan process. C-scan is a subset of F-scan, the C-scan looking only at one principal feature, amplitude. Further information about ultrasonic testing can be found in references (q) and (t).

III. EQUIPMENT

A. The F-scan system utilizes a computer-based system with a graphics terminal, analog-to-digital (A/D) converter, ultrasonic pulser/receiver, a computer-controllable x-y scanner, an oscilloscope, and ultrasonic transducers. A block diagram of the system is shown in Figure 1, with a description of each piece below.

1. PDP-11/05 MINICOMPUTER. This is a 16-bit computer with 64 k bytes of memory, RK05 hard disk, and dual floppy disks. This is equipped with interface cards to control the A/D converter, x-y scanner, graphics terminal, and pulser/receiver unit. The programs that collect and store the data are written in FORTRAN and the control programs are written in MACRO assembly language.

2. GRAPHICS TERMINAL. A Tektronix 4014 graphics terminal is used to display the F-scans and ultrasonic waveforms. The terminal has 1024 by 780 dot matrix with vector capability. A Tektronix 4631 hard copy unit is connected for permanent recording.

3. ANALOG-TO-DIGITAL CONVERTER. A Biomation 8100 transient recorder is used to capture the ultrasonic waveform. It can store up to 2048 samples at 100 MHz (every .01 μsec) with 8-bit resolution (256 quantum levels).

4. ULTRASONIC PULSER/RECEIVER. A KB6000 computer-controllable flaw detector is used to pulse the transducer and receive and amplify the ultrasonic signal. This unit has programmable functions such as gain and gate settings which are useful in data acquisition.

5. X-Y SCANNER. This unit positions the transducer over the specimen. The computer sends the desired position to the x-y scanner controller which tells the stepped motor to move the transducer into place. The minimum scanning increment is .01 inch.

6. ULTRANSONIC TRANSDUCER. Various transducers are available for inspection. Nominal frequencies used are 2.25, 5.0, and 10.0 MHz while diameters and focal distances are varied.

B. The scanning procedure is discrete; that is, data is taken for individual points. The spacing between points depends on the size of the defects, the size of the specimen, and ultrasonic beam width. Obviously a small scanning increment distance is desired; however, since each point takes a fixed time, the fewer points taken hastens the process. After the area to be scanned and the scanning increment have been determined, the data collection starts. First the gain is adjusted so the maximum number of quantum levels in the A/D are utilized. The signal is gated and 5 μsec (500 points) of the signal is transferred to the computer. The signal is averaged four times to eliminate noise and is then stored on a disk. The transducer is then moved to the next position and the process begins again.

IV. TEST PROCEDURE

A. After developing the F-scan system further, the technique was applied to a sample repair patch of composite (0/90/+45) which was obtained from the Naval Air Development Center (NAVAIRDEVCEN). A 11-inch-diameter circular patch with a variable thickness (0.125 to 0.024 inch) was scanned. As expected, penetration of an ultrasonic wave through the defected patch was difficult. Areas of high attenuation of the signal were noticed upon preliminary testing. Different kinds of defects were suspected to exist in the patch—defects such as debondings, delamination, and porosity and void content. However, the primary goal of this study was to develop an algorithm that could predict the gross defects within the patch that were critical to the structural performance, regardless of the defect type, so that guidelines for composite patch repair could be formulated.

B. An immersion ultrasonic pulse echo method was used for this study. In this technique, the sample was scanned in a tank of water utilizing one transducer both as sender and receiver. An ultrasonic wave passed through a water path before impinging on the composite patch surface. Since the patch itself was thin, it was difficult to distinguish between the first defect echo and front wall echo; therefore, the entire signal was gated, digitized, and stored in the computer.

C. The second method was the use of a reflector plate where the sound beam passed through the water patch to the sample, then to the reflector plate and back to the search unit. In the case of lower attenuative materials it was advantageous to use this technique, because it resulted in greater signal changes for gating and recording the ultrasonic signals. We also studied reflector-plate analysis to see how it performed with F-scan analysis on the composite. The patch was scanned several times with different frequency transducers ranging from 2.25 MHz to 10 MHz which are commercially available from KB-Aerotech. The low signal-to-noise ratio and high gain capabilities were considered as the main criteria in selecting these transducers. Low-frequency transducers have a better penetration ability than high-frequency transducers. However, the resolution capability reduces as the frequency values decrease.

D. Taking all of these into consideration, the patch was scanned with 2.25, 5, and 10 MHz transducers. The scanning increment distance was 0.05 inches in the X-Y direction. The scanning was done along the lines parallel to the X axis and 1-3/4 and 2-1/2 inches away from the center of the patch.

E. The wave speed in the material was calculated to be 0.060 inch/μsec. The thickest part of the specimen was 3/16 inch. Therefore, the time it took for the sound to pass through the specimen was 3.1 μsec. The Biomation 8100 transient recorder's minimum sample rate (.01 μsec) was used since it gives the best frequency resolution. Therefore at least 310 data points must be taken to record the entire echo returning from the specimen. To include the backwall echo, at least 400 data points (4.0 μsec) must be taken. A Fast Fourier

Transform algorithm has 2^n points where n is an integer. The value of n used is 9 (512 points) which is 5.12 μsec of data.

F. When attempting to find features that would be useful in detecting defects, destructive analysis of the specimens must be done. The damage content was therefore determined by making photomicrographs of the specimens. Extreme care had to be taken so that no damage would be induced in the samples while preparing (cutting, mounting, and polishing) the specimens for photomicrographs. A sample photomicrograph is shown in Figure 2.

V. F-SCANNING

A. Ultrasonic F-scanning, which stands for feature scanning, is an extension of the traditional C-scan. In C-scan, the only feature considered is the amplitude of the ultrasonic signal, whereas in F-scan, any number of features can be considered. In the F-scan data acquisition system, the entire ultrasonic signal is digitized and stored on a magnetic disk by a computer. This data file can be recalled at any time for feature extraction and analysis.

B. The critical point in F-scan analysis is feature extraction. Since the raw signal has been stored, any time domain feature can be examined, such as peak amplitude (like C-scan) root mean squared (RMS) value, rise time of the signal, pulse duration, etc. The frequency spectrum of the raw signal can be acquired by utilizing a Fast Fourier Transform (FFT) routine. This enables the analysis of many frequency domain features such as peak frequency, 6 db bandwidth, attenuation in certain bands, frequency shift, etc. Other features of a more statistical nature can be selected such as skewness, moments of inertia, etc. Also the signals can be transformed into other domains such as the cepstral domain. The analysis was limited to just time and frequency domain features since their physical properties are easier understood and are more field applicable. Ten features were selected for this study. The first five features are time domain features. The ratio of amplitudes is often a more accurate feature since the effects of surface condition are cancelled out. No time domain features other than features 1 through 5 (such as rise time, fall time, or pulse duration) were examined since it was difficult to localize individual defect echoes because of the thinness of the composite and the high noise level associated with it. The remaining 5 features deal with frequency domain. Whenever working in the frequency domain, the power spectrum has been normalized so that the area equals one. Therefore, any area measurements of frequency content between two frequencies always corresponds to the percent of the area of the spectrum.

FEATURE	DISCUSSION
1. Peak amplitude of RF signal	This is the basic C-scan feature
2. Root mean squared (RMS) value of the ultrasonic pulse	Since the signal was digitized, each point is considered with the following equation: $$RMS = \frac{1}{n} \sum_{i=1}^{n} x_i^2$$ where n = number of samples (512) and x is the number of quantum levels.
3. The ratio of feature 1 to feature 2	None
4. Peak amplitude of back-wall echo	None
5. Peak-to-peak ratio between the first echo (feature 1) and the backwall echo (feature 4)	None
6. The percentage frequency content from a low frequency value to the nominal mid-frequency value of the transducer	Features 6 and 7 deal with area measurement. In explaining feature 6, for example, the F-scanning was done with a 10.0 MHz transducer, the percent frequency content would be measured from 2 MHz to 10 MHz. The low value of 2 MHz was chosen to eliminate any low frequency noise that might enter in.
7. Percentage of frequency content from the nominal mid-frequency value to a high frequency value	Feature 7: Again, for 10 MHz probe, the area would be taken from the mid-frequency of 10 MHz to an upper frequency of 18 MHz so that the high frequency noise was not considered. These two features (6,7) were used to detect spectral shifts. The frequency spectrum for all transducers used were symmetric with respect to the center frequency of the ultrasonic pulse, which was then from a flat smooth reflector as reference. Attenuation of higher frequencies would result in a decrease in feature value for feature 6 and increase in value for feature 7.

FEATURE	DISCUSSION
8. Ratio of feature 6 to feature 7	This feature shows the frequency shift. As the frequency shift increases, so does the feature value. The frequency spectrum was also broken into 1 MHz bands and examined. The feature values showed similar classifying characteristics as features 6, 7, and 8 and were not pursued.
9. Peak frequency of the ultrasonic pulse	This feature also can be used to detect changes in the spectrum.
10. Similarity coefficient between a reference signal and the ultrasonic signal	This feature is called a similarity measure which compares the spectrum of the reference pulse to the spectrum of signal from the composite. This technique is also referred to as matched filtering. The following formula was employed where F1 is the reference spectrum and F2 is the spectrum from the composite: $$S = \sum_{i=1}^{n} \frac{(F1_i) \times (F2_i)}{(F1_i)^2 + (F2_i)^2 - (F1_i) \times (F2_i)}$$ For this, a perfect similarity is a 1 and no similarity is a 0.

C. Now that features have been extracted, the analysis of these features must begin. An example of the procedure is described next.

1. The specimen was scanned as described in the procedure section with a 3-by-20 matrix of data points. The ratio of the area below mid-frequency to the area above the mid-frequency, feature 8, is analyzed. A 2.25-MHz transducer was used. A photomicrograph showed that the lower part of the composite has severe defects, the rest of the specimen is relatively good.

2. In the first part of the analysis, the raw feature values are examined to see if there is any correlation between these and the photomicrograph. Figure 3 shows the raw data. Notice that the last four rows have feature values around 0.7 or more and the good area feature values are around 0.6 or less.

NAEC-92-159

3.   In the next part of the analysis, a histogram of the data is plotted
to help better define the threshold used in classifying defects. In the his-
togram, also shown in Figure 3, the data is fairly uniformly distributed with
a majority of the feature values falling between 0.54 and 0.62. In the final
step, a threshold is selected and an F-map is drawn showing the bad areas in
white and the good areas in black. In Figure 3, an F-map is drawn with a
threshold of 0.62. This threshold definitely picks out the bad areas; how-
ever, some areas considered good by the micrograph were also designated bad in
an F-map.

4.   Looking at the raw feature values again, the points missed are very
close to the threshold and probably are marginal areas that could be con-
sidered good but should be frequently re-examined. The question of how sensi-
tive the threshold should be is always a problem. One must consider the
criticality of the defect. This is a criterion that must be determined by
evaluating flaw type, flaw size, expected life, specimen loading, fatigue
history, and other engineering factors. When this is determined, a proper
threshold can be selected.

5.   A technique called spacial integration is used to help increase accu-
racy in the defect location process. This technique follows the same philos-
ophy as the signal averaging to help eliminate signal noise in that it con-
siders the neighboring points when calculating the feature value. Two tech-
niques that can be employed are described next. The first integration method,
called the square method, uses the equation

$$\frac{1}{4h^2} \iint_s f(x,y)\, dxdy = \sum_{i=1}^{n} w_i\, f\,(x_i y_i)$$

where the weights w_i are given by
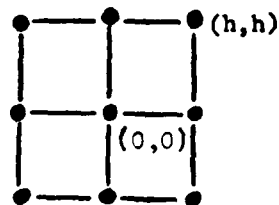
$(x_i,\ y_i)$	w_i
(0, 0)	4/9
$(\pm h,\ \pm h)$	1/36
$(\pm h,\ 0)$	1/9
$(0,\ \pm h)$	1/9

12

This technique gives the most weight to the center feature ($f(0, 0)$) and decreasing importance as you get farther away. The total sum of the weights add up to one. The second technique, called the Laplacian, takes the gradient of the feature space using the equation

$$\nabla^2 f_{0, 0} = \left(\frac{\partial^2 f}{\partial x^2} + \frac{\partial^2 f}{\partial y^2}\right)_{0, 0}$$

$$= \frac{1}{h^2} (u_{1, 0} + u_{0, 1} + u_{1, 0} + u_{0, -1} - 4u_{0, 0}) + 0(h^2)$$

diagrammatically
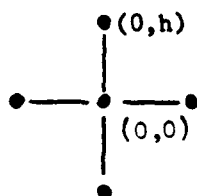
This technique can be extended to more feature points on the x and y axes. These techniques cannot be done on the endpoints; therefore, only the middle point can be calculated. For the 20 x 3 data matrix used in this examination, the data was reduced to an 18 x 1 matrix for data points 2 through 19. This data reduction helps with the picking of thresholds and evaluation of the data.

VI.   RESULTS

A. GENERAL. The results are broken into three sections. The first section is on transducer selection, the second is on F-scan system accuracy, and the third is the results of the F-scanning on defect location in the composite patch. These results are described next.

B. TRANSDUCER SELECTION. In our evaluation, the lower frequency transducer gave the best results. This is mainly due to the better penetration capabilities of the low frequencies (see ultrasonic background section). Figure 4 shows ultrasonic waveforms from the same section of the patch for a 2.25-, 5-, and 10-MHz transducer. The time in the composite from the front to the back of the composite is 3.1 μsec, which is designated on the waveform. On the signals acquired with the 2.25-MHz probe, a backwall echo can be seen, whereas with the 5-MHz and 10-MHz probes very little signal can be detected after the front wall echo. A defect cannot be detected if the sound does not penetrate at least to the defect. Therefore a 2.25-MHz transducer works better for finding defects with all features attempted. The only disadvantage in using a low-frequency transducer is the low axial resolution of the transducer. However, we were trying to find damage in the patch, not which ply it occurred at. If the position is critical, only defective areas would have to be re-evaluated.

C. F-SCAN SYSTEM ACCURACY

1. In an attempt to determine system accuracy and precision, a sample of graphite epoxy (thickness = 0.05 inch) with an artificial edge slit of about 0.06 inch was scanned in the early stage of the project. The fact that the movement of the scanning arm was controllable in the x-y directions with a minicomputer, enabled us to scan the slit at different increments (0.05 to 0.03 inch).

2. The results are shown in Figure 5 for different features using the spacial integration technique. Each block in Figure 5 is 0.03 inch, thus the expected number of blocks for a slit of 0.06 inch would be two in the x (vertical) direction which the F-scans in the figures show. These results are the evidence of the F-scanning system's sharpness in predicting the slit location. However, the results without spacial integration showed a slit of double width (0.12 inch) which means some improvements could be made to the system. A better focusing has to be developed to further ensure the sharpness of the system. Use of small probes results in a better resolution which in turn affects the results directly. As has been the case in the past, averaging techniques could further improve the system, too.

D. F-SCANNING OF PATCH

1. A large amount of the work effort was centered in the evaluation of features in their defect location capabilities. As can be expected, some features did perform better than others. Of the featues described in the F-scan section, features 5 through 8 performed better than the others. The first four features (1 through 4), which were time domain features, did not work as well since they are highly dependent on the surface condition of the composite. Feature 9, peak frequency, was somewhat successful but not as successful as the frequency shift (feature numbers 6, 7, and 8). Feature 10, similarity co-efficient, was not successful mainly because there were very few defect-free areas to which this measure is overly sensitive.

2. In the analysis, the patch was scanned, cut, and photomicrographed as previously described. The photomicrographs were examined to determine good and bad areas. This classification was based on the void content, the bad having significant void content in comparison to the good areas which still had some void content. Figure 6 shows three photomicrographs of specimen A. The first photomicrographs shows severe void content and would be classified as a bad area of the specimen. The second picture shows smaller voids; however, this is still considered a bad area because of the multiple voids. The third is from a good area; note that there is still some small void content. There were no areas that could be considered defect free; so "good" is just a relative measurement. In the analysis process, first the optimum thresholds of the F-scan were selected by comparing the F-scan and micrographs, and moving the threshold up or down until the F-scan and micrograph corresponded identically or as

closely as possible. This threshold was then applied to the other specimens and an F-scan was generated. This F-scan was compared to the micrograph, and sensitivity and specificity measures were calculated. The sensitivity is the percentage of the bad areas correctly found and the specificity is the percentage of the good areas correctly found. In our analysis, the thresholds were adjusted so that the bad areas were more reliably found, thus increasing the sensitivity. However, this threshold would designate some good areas bad, thus decreasing the specificity. This adjustment of the threshold depends on the surface, loading, fatigue, etc., of the specimen.

3. Three samples were scanned, cut, and micrographed. The good and bad areas were defined as shown in Figure 7. The four best features are evaluated using the following procedure. First the optimum threshold is selected using specimen A. The sensitivity and specificity are determined using specimens B and C, and are shown in Table 1. These indexes of performances are summarized in Table 2. The evaluation of each of the features follows.

  a. **Feature 5: Peak-to-Peak Ratio**

   (1) This feature is the ratio of the peak amplitude of the first signal to the peak amplitude of the backwall echo. The size of the backwall echo is a measure of the sound energy that has passed through the entire composite. If there is a large void, the sound energy would return earlier in time. Also, the attenuation was more severe with the bad composite, thus making the backwall echo smaller. The first peak signal is used to help compensate for surface conditions. If the surface is rough at a particular place, the sound energy will be scattered, thus less energy will get to the backwall. However, the first reflection will also be smaller, so dividing the backwall echo by the first echo gives a more accurate value measure of the quality of the composite.

   (2) Figure 8 shows the feature values and F-scans for composite specimen A for both the point-by-point analysis and for spacial averaging. This specimen was used to set the threshold which was defined as 0.093. Areas above that threshold were considered good since this corresponds to higher backwall echoes and below this value were considered bad. This threshold was evaluated on specimens B and C. The results are displayed in Figures 9 and 10. The overall sensitivity is 58/96 (60%) and specificity is 64/84 (76%) for this feature. The individual and overall results are shown in Tables 1 and 2.

  b. **Features 6, 7, and 8: Frequency Shift**

   (1) These three features are used to detect shifts in the frequency spectrum. Feature 6 is the percentage of frequency content below the mid-frequency of the transducer (2.25 MHz). Feature 7 is the percentage of frequency content above the mid-frequency of the transducer. Feature 8 is the ratio of Feature 6 to Feature 7. The basic physical principle of this feature is as the ultrasonic beam passes through the composite, the higher

frequencies will be attenuated faster. If the sound beam encounters a large interface such as an air-filled void, the ultrasonic wave will travel through less composite and be sharply reflected, thus causing less high-frequency attenuation. Therefore a shift in the frequency spectrum towards lower frequencies signifies a good composite. This corresponds to an increase in frequency content below the mid-frequency (Feature 6), a decrease in frequency content above the mid-frequency (Feature 7), and an increase in the ratio (Feature 8). As before, the threshold was set with specimen A and tested with specimens B and C. The threshold was 0.32 for Feature 6, 0.50 for Feature 7, and 0.59 for Feature 8. The feature values add F-scans for these features and specimens are shown in Figures 11 through 19. The corresponding sensitivity and specificity are shown in Table 1.

(2) The overall sensitivity was 78.6% (302/284) with a specificity of 82% (276/336). With the spacial integration techniques, the sensitivity improved to 85.8% (103/120) with a specificity of 89.6% (86/96). These results are summarized in Table 2. These are fairly good results; however, it must be remembered that this is a fairly limited study. Only one patch was examined; therefore, changes from patch to patch cannot be studied.

VII. CONCLUDING REMARKS AND RECOMMENDATIONS

A. A new ultrasonic tool, called F-scan, has been developed to locate defects in composite materials. F-scan is an extension of C-scan in which many features are examined, not just amplitude. This tool demonstrated excellent potential in the inspection of composite patches, where normal C-scan methods proved unsuccessful. Here, four features were successfully used to locate defects in the patch with 85% accuracy. This was a very limited study where only certain sections of one composite patch were examined. Therefore, no universal testing procedures were developed, only general guidelines for future work were established.

B. In the development of a new inspection procedure, it is critical to have a good selection of specimens for analysis. It is absolutely necessary to cooperate with the manufacturer so good representative defects can be obtained. Also the final user must help define the criteria for defect criticality. This is the only way a complete F-scan system can be ascertained.

C. Tools are now available to assist us in the solution of many specific problems in composite materials and composite repair.

VIII.   REFERENCES

(a) Grimes, G. C., "Experimental Study of Compression-Compression Fatigue of Graphite Epoxy Composites," ASTM-STP 734, American Society for Testing and Materials, 1981, pp. 281-337.

(b) Komishi, D. Y. and Johnston, W. R., "Fatigue Effects of Delaminations and Strength Degradation in Graphite Epoxy Laminates," ASTM-STP 674, American Society for Testing and Materials, pp. 590-619.

(c) Theocaris, P. S. and Stassinakis, C. A., "Crack Propagation in Fibrous Composite Materials Studied by SEM," J. Composite Materials, Vol. 15, March 1981, p 133.

(d) Wang, S. S., "Delamination and Crack Growth in Unidirectional Composites Under Static and Cyclic Loading," ASTM-STP 674, American Society for Testing Materials, 1977, pp. 642-663.

(e) Miller, A. G. and Wingert, A. L., "Fracture Surface Characterization of Commercial Graphite Epoxy Systems," ASTM-STP 696, American Society for Testing and Materials, 1979, pp. 223-273.

(f) Sheldon, W. H., "Comparative Evaluation of Potential NDE Techniques for Inspection of Advanced Composite Structure," Materials Evaluation, Vol. 36, 1978, pp. 41-46.

(g) Hagemairer, D. J., Fassbender, R. H., "Nondestructive Testing of Advanced Composites," Materials Evaluation, Vol.   , 1979, pp. 43-49.

(h) Kaelble, D. H. and Dynes, P. J., "Nondestructive Testing for Shear Strength Degradation of a Graphite Epoxy Composite," ASTM-STP 617, American Society for Testing and Materials, 1977, pp. 190-200.

(i) Williams, F. H. and Doll, B., "Ultrasonic Attenuation as an Indicator of Fatigue Life of Graphite Fiber Epoxy Composite," Materials Evaluation, 1980, pp. 33-37.

(j) Hayford, D. T. and Henneke, E. G. II, "A Model for Correlating Damage and Ultrasonic Attenuation in Composites," ASTM-STP 674, American Society for Testing and Materials, 1979, pp. 184-200.

(k) Williams, J. H. and Lampert, N. R., "Ultrasonic Evaluation of Impact-Damaged Graphite Fiber Composite," Materials Evaluation, December 1980, pp. 68-72.

(l) Daniel, M. I. and Schramm, S. W. and Libert, T., "Fatigue Damage Monitoring in Composite by Ultrasonic Mapping," Materials Evaluation, Vol. 39, 1981, pp. 834-839.

(m) Carson, J. M. and Rose, J. L., "An Ultrasonic Nondestructive Test Procedure for the Early Detection of Fatigue Damage and the Prediction of Remaining Life," Materials Evaluation, April 1980, pp. 27-33.

(n) Gerick, D. R., "Ultrasonic Spectroscopy,"(3H6) Proceedings of the Eighth World Conference on Nondestructive Testing," September 1976.

(o) Rose, J. L., Carson, J. M. and Leidel, D. J., "Ultrasonic Procedures for Inspecting Composite Tubes," ASTM-STP 551, American Society of Testing and Materials, 1973, pp. 311-325.

(p) Mucciardi, A. N., et al., "Adaptive Nonlinear Signal Processing for Characterization of Ultrasonic NDE Waveforms, Task 1 - Inferences of Flat Bottom Hole Size," AFML Interim Report, Contract number F33615-74-C-5122.

(q) Rose, J. L. and Goldberg, B. B., Basic Physics in Diagnostic Ultrasound, John Wiley & Sons, Inc., New York, 1980.

(r) Rose, J. L., Avioli, M. J. and Jeong, Y. H., "Utility of a Probability Density Function Curve and F-maps in Composite Material Inspection," presented at the Spring meeting of ASNT in Philadelphia, March 1980, and to be published in Experimental Mechanics, April 1982.

(s) Agarwal, D. B. and Broutman, L. J., Analysis and Performance of Fiber Composites, John Wiley & Sons, Inc., New York, 1976.

(t) Krautkramer, J. and Krautkramer, H.,"Ultrasonic Testing of Materials," Second Edition - Translation, Springer-Verlag, Inc., New York, 1969.

TABLE 1 – RESULT OF COMPOSITE PATCH STUDY
(Sensitivity and specificity for specimens A, B, and C,
before and after spacial integration)

WITHOUT SPACIAL INTEGRATION

FEATURE 5

	A	B	C	TOTAL
Sensitivity	$\frac{20}{36}$ = 55%	$\frac{15}{30}$ = 50%	$\frac{23}{30}$ = 76%	$\frac{58}{96}$ = 60%
Specificity	$\frac{15}{24}$ = 62%	$\frac{26}{30}$ = 87%	$\frac{23}{30}$ = 77%	$\frac{64}{84}$ = 76%
Overall	$\frac{35}{60}$ = 58%	$\frac{41}{60}$ = 68%	$\frac{46}{60}$ = 77%	$\frac{122}{180}$ = 68%

FEATURE 6

	A	B	C	TOTAL
Sensitivity	$\frac{33}{36}$ = 92%	$\frac{19}{30}$ = 63%	$\frac{27}{30}$ = 90%	$\frac{79}{96}$ = 82%
Specificity	$\frac{16}{24}$ = 67%	$\frac{30}{30}$ = 100%	$\frac{28}{30}$ = 93%	$\frac{74}{84}$ = 88%
Overall	$\frac{49}{60}$ = 81%	$\frac{49}{60}$ = 81%	$\frac{55}{60}$ = 92%	$\frac{153}{180}$ = 85%

FEATURE 7

	A	B	C	TOTAL
Sensitivity	$\frac{35}{36}$ = 97%	$\frac{29}{30}$ = 97%	$\frac{29}{30}$ = 97%	$\frac{93}{96}$ = 97%
Specificity	$\frac{15}{24}$ = 62%	$\frac{23}{30}$ = 77%	$\frac{21}{30}$ = 70%	$\frac{59}{84}$ = 67%
Overall	$\frac{50}{60}$ = 83%	$\frac{57}{60}$ = 87%	$\frac{50}{60}$ = 83%	$\frac{152}{180}$ = 84%

FEATURE 8

	A	B	C	TOTAL
Sensitivity	$\frac{28}{36}$ = 78%	$\frac{17}{30}$ = 57%	$\frac{27}{30}$ = 90%	$\frac{72}{96}$ = 75%
Specificity	$\frac{20}{24}$ = 83%	$\frac{30}{30}$ = 100%	$\frac{29}{30}$ = 97%	$\frac{79}{84}$ = 94%
Overall	$\frac{48}{60}$ = 80%	$\frac{47}{60}$ = 78%	$\frac{56}{60}$ = 93%	$\frac{151}{180}$ = 84%

TABLE 1 (CONTINUED) - RESULT OF COMPOSITE PATCH STUDY
(Sensitivity and specificity for specimens A, B, and C,
before and after spacial integration)

WITH SPACIAL INTEGRATION

FEATURE 5

	A	B	C	TOTAL
Sensitivity	$\frac{9}{11}$ = 82%	$\frac{5}{9}$ = 55%	$\frac{8}{10}$ = 80%	$\frac{22}{30}$ = 73%
Specificity	$\frac{6}{7}$ = 86%	$\frac{9}{9}$ = 100%	$\frac{7}{8}$ = 87%	$\frac{22}{24}$ = 92%
Overall	$\frac{15}{18}$ = 83%	$\frac{14}{18}$ = 78%	$\frac{15}{18}$ = 83%	$\frac{44}{54}$ = 81%

FEATURE 6

	A	B	C	TOTAL
Sensitivity	$\frac{11}{11}$ = 100%	$\frac{7}{9}$ = 78%	$\frac{9}{10}$ = 90%	$\frac{27}{30}$ = 90%
Specificity	$\frac{5}{7}$ = 71%	$\frac{9}{9}$ = 100%	$\frac{8}{8}$ = 100%	$\frac{22}{24}$ = 92%
Overall	$\frac{16}{18}$ = 89%	$\frac{16}{18}$ = 89%	$\frac{17}{18}$ = 94%	$\frac{49}{54}$ = 91%

FEATURE 7

	A	B	C	TOTAL
Sensitivity	$\frac{11}{11}$ = 100%	$\frac{9}{9}$ = 100%	$\frac{10}{10}$ = 100%	$\frac{30}{30}$ = 100%
Specificity	$\frac{5}{7}$ = 71%	$\frac{6}{9}$ = 67%	$\frac{7}{8}$ = 87%	$\frac{18}{24}$ = 75%
Overall	$\frac{16}{18}$ = 89%	$\frac{15}{18}$ = 83%	$\frac{17}{18}$ = 94%	$\frac{48}{54}$ = 89%

FEATURE 8

	A	B	C	TOTAL
Sensitivity	$\frac{9}{11}$ = 82%	$\frac{6}{9}$ = 67%	$\frac{9}{10}$ = 90%	$\frac{24}{30}$ = 80%
Specificity	$\frac{7}{7}$ = 100%	$\frac{9}{9}$ = 100%	$\frac{8}{8}$ = 100%	$\frac{24}{24}$ = 100%
Overall	$\frac{16}{18}$ = 89%	$\frac{15}{18}$ = 83%	$\frac{17}{18}$ = 94%	$\frac{48}{54}$ = 89%

TABLE 2 - OVERALL INDEXES OF PERFORMANCE
(All Features Combined)

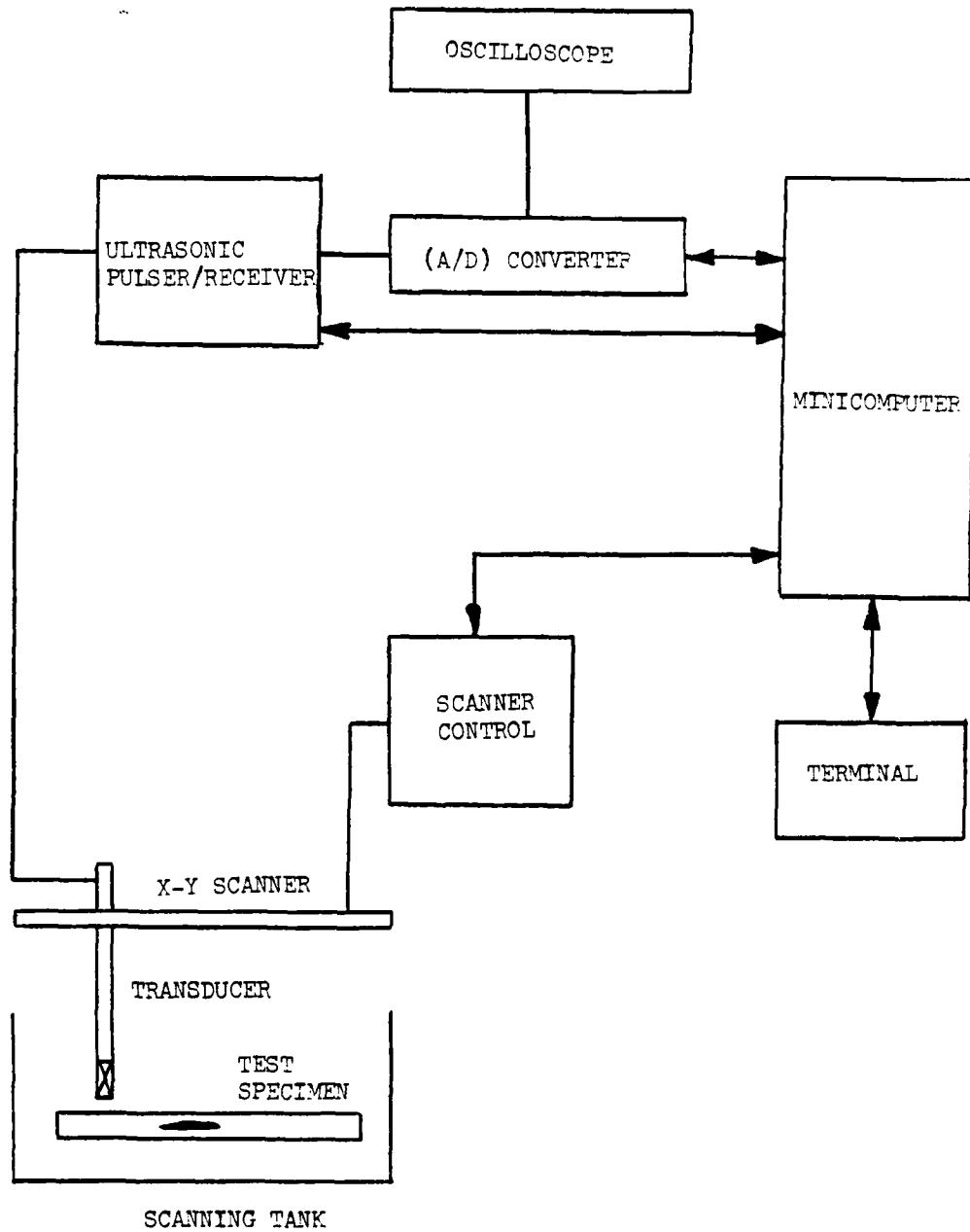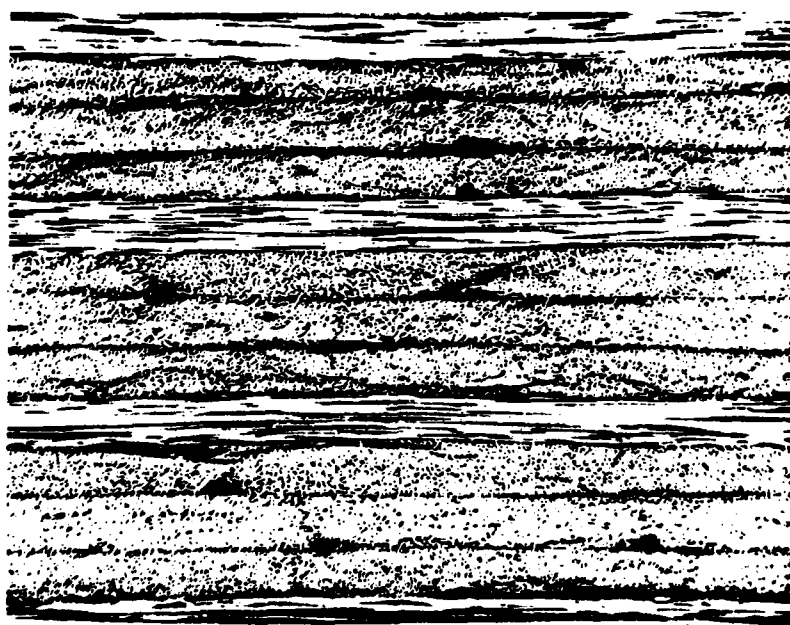|	Individual Point Data	Spacial Integration Data
Sensitivity	$\frac{302}{384}$ = 78.6%	$\frac{103}{120}$ = 85.8%
Specificity	$\frac{276}{336}$ = 82%	$\frac{86}{96}$ = 89.6%
Overall	$\frac{578}{720}$ = 80.2%	$\frac{189}{216}$ = 87.5%

Figure 1. Block Diagram of the Data Acquisition System

Figure 2. Sample Photomicrographs

23

Bad

Good

ENTER THRESHOLD VALUE: .62

0.39   0.47   0.54   0.62   0.69   0.77   0.85

24
22
20
18
16
14
12
10
8
6
4
2

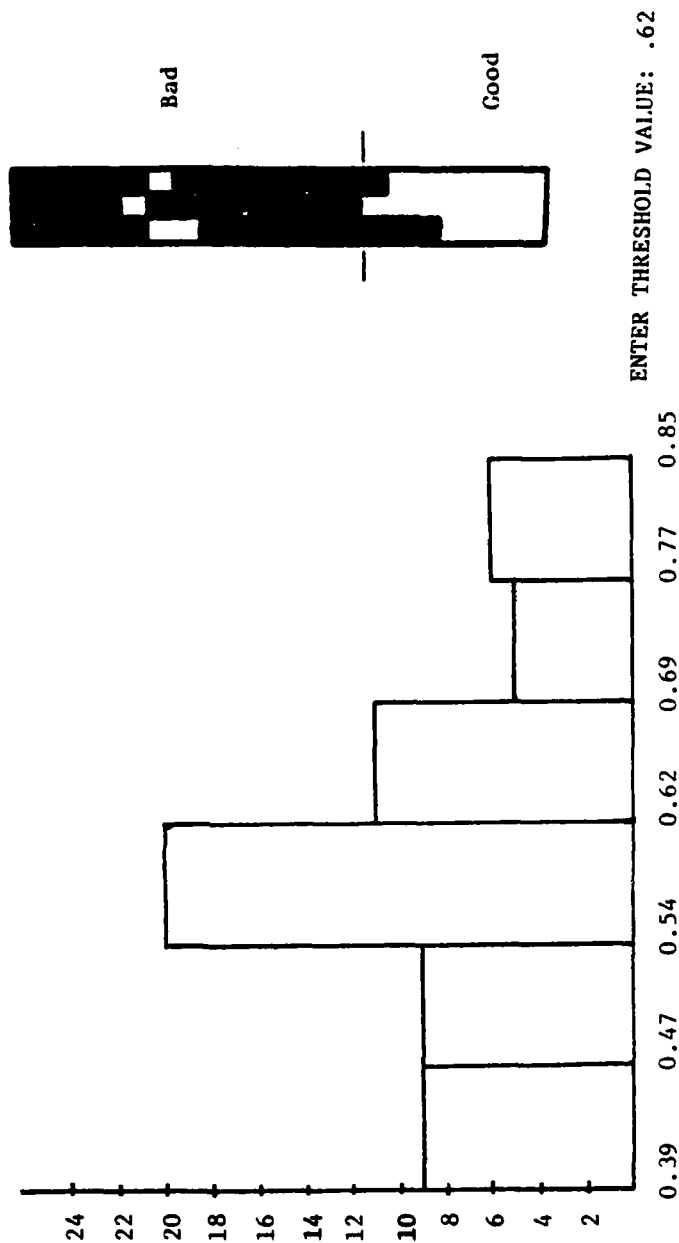|			
0.4134	0.3893	0.4214	
0.4214	0.4224	0.4652	
0.4198	0.5777	0.5142	
0.5088	0.5989	0.5912	
0.6044	0.6254	0.6171	
0.6491	0.5894	0.6421	
0.6333	0.5426	0.5707	
0.5812	0.4976	0.5162	
0.5462	0.4973	0.4629	
0.5365	0.5376	0.4518	
0.5489	0.5605	0.4964	
0.5697	0.5824	0.5322	
0.5559	0.6195	0.5620	
0.5727	0.6493	0.5937	
0.5603	0.6816	0.6750	
0.6142	0.7595	0.7786	
0.6825	0.8363	0.8477	
0.7436	0.7908	0.8439	
0.7419	0.7130	0.8895	
0.6911	0.6404	0.7075	

Figure 3. Raw Data, Histogram, and F-map of Feature 8, Ratio of Feature 6 to Feature 7
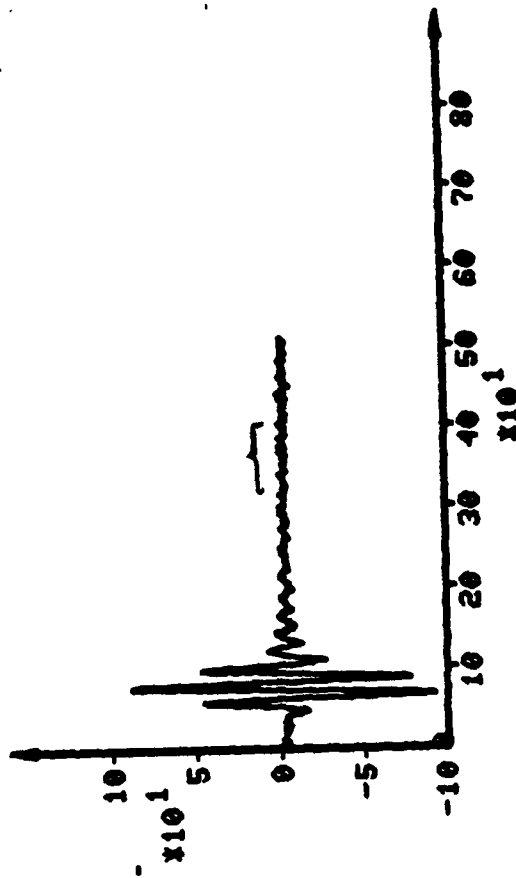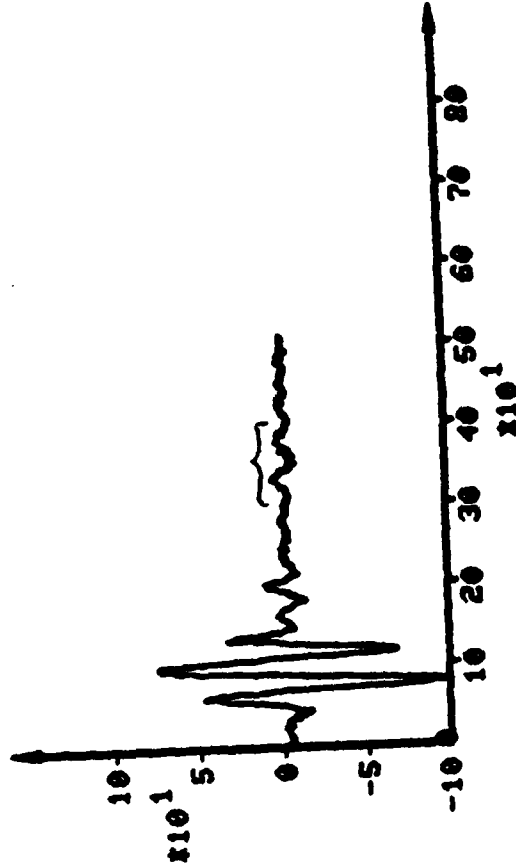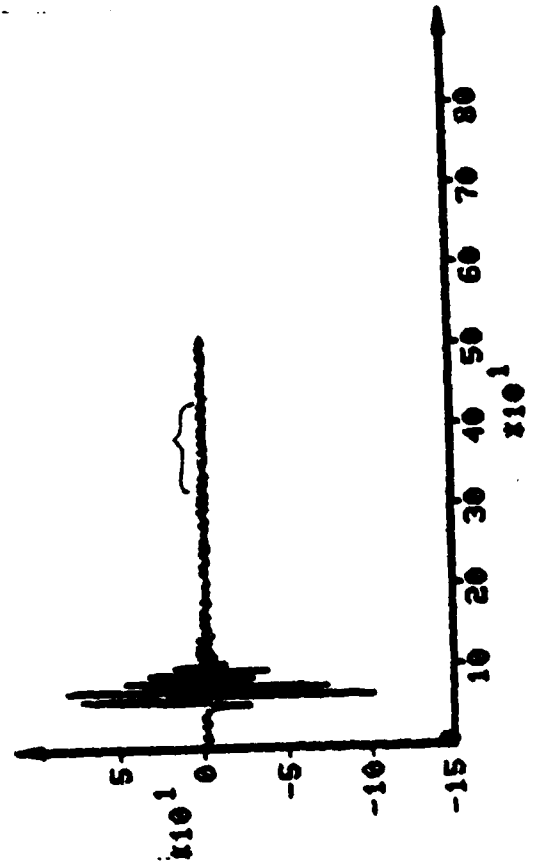
Figure 4. Comparison of Waveforms taken from the Same Point with Different Frequency Transducers

a) 2.25 MHz

b) 5.0 MHz

c) 10.0 MHz

25

FEATURE 5   FEATURE 6   FEATURE 7   FEATURE 8
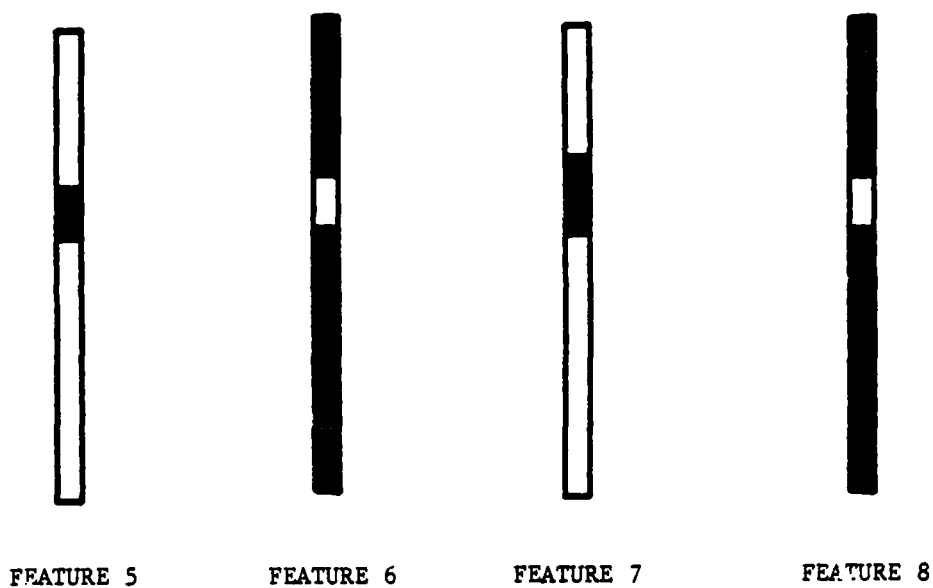
Figure 5. Result of F-scanning a Slit

26

Figure 6. Micrograph of a Sample with a Major Delamination (a, b), Relatively Good Sample

Specimen C   Specimen B   Specimen A
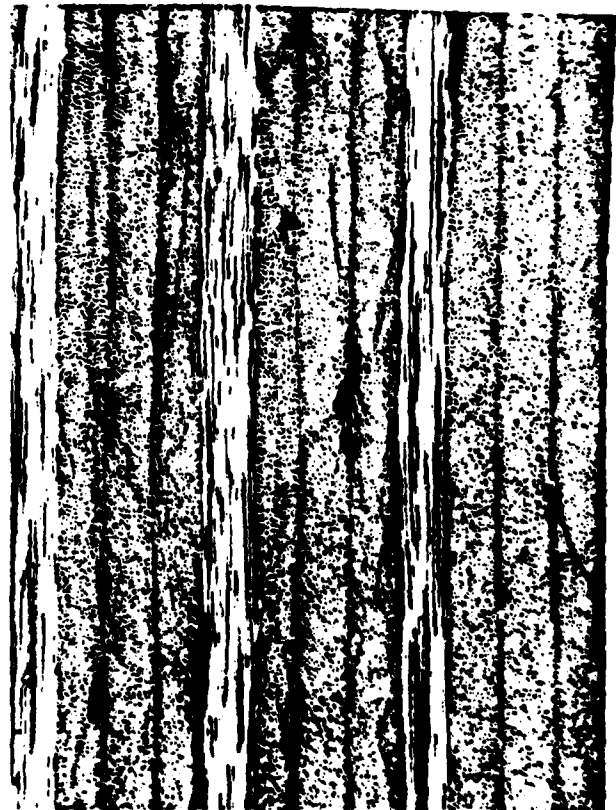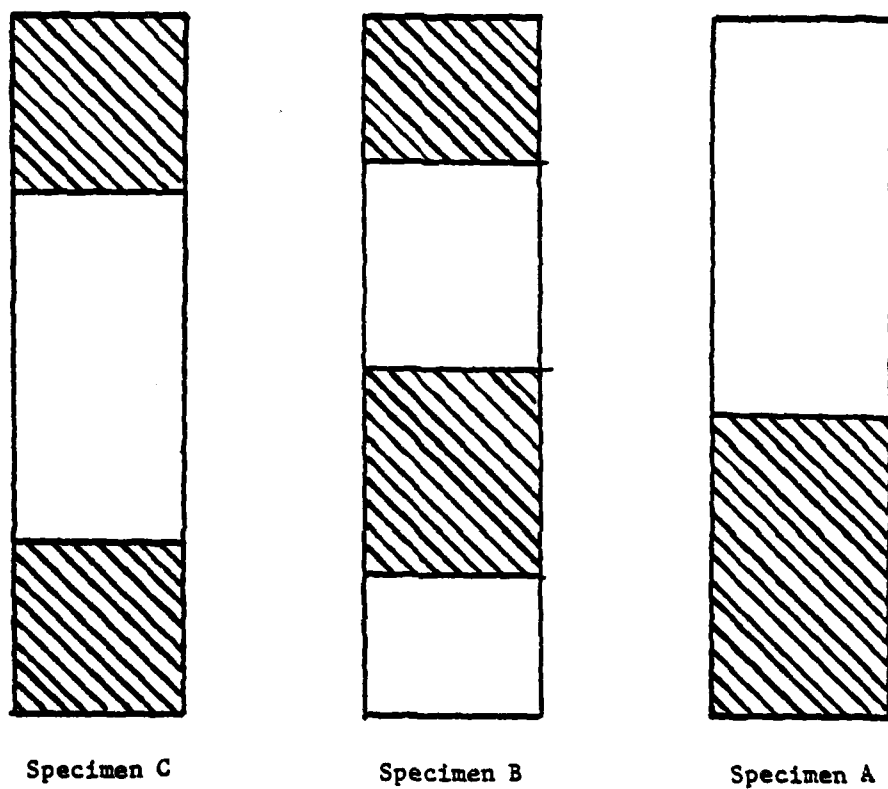
☐ Bad Area

▨ Good Area

Figure 7. Schematic of Good and Bad Areas of Sample Specimens

28

Bad

Good

spacial integration
data

Black – Bad
White – Good

Threshold = .093

0.0904
0.0986
0.0952
0.0900
0.0752
0.0704
0.0717
0.0702
0.0728
0.0793
0.0867
0.0966
0.1121
0.1195
0.1173
0.1106
0.0939
0.0760

Bad

Good

Individual point
data

Figure 8. Feature 5, Peak-to-Peak Ratio of Front Echo to Backwall Echo
(Specimen A, used to set threshold).

Good

Bad

Good

Bad

spacial integration
data

0.1056
0.1087
0.1113
0.1061
0.1092
0.0974
0.0900
0.0921
0.1013
0.1173
0.1259
0.1245
0.1297
0.1254
0.1006
0.0758
0.0633
0.0712

Black - Bad
White - Good

Threshold = .093

Good

Bad

Good

Bad

individual data
points

Figure 9. Feature 5, Peak-to-Peak Ratio of Front Echo to Backwall Echo (Specimen B used to test threshold).

Good

Bad

Good

spacial integration
data

0.1275
0.1167
0.1037
0.0875
0.0721
0.0774
0.0824
0.0738
0.0812
0.0836
0.0868
0.0923
0.0993
0.0968
0.0945
0.1051
0.1197
0.1222

Black — Bad
White — Good

Threshold = .093

Good

Bad

Good

Individual point
data
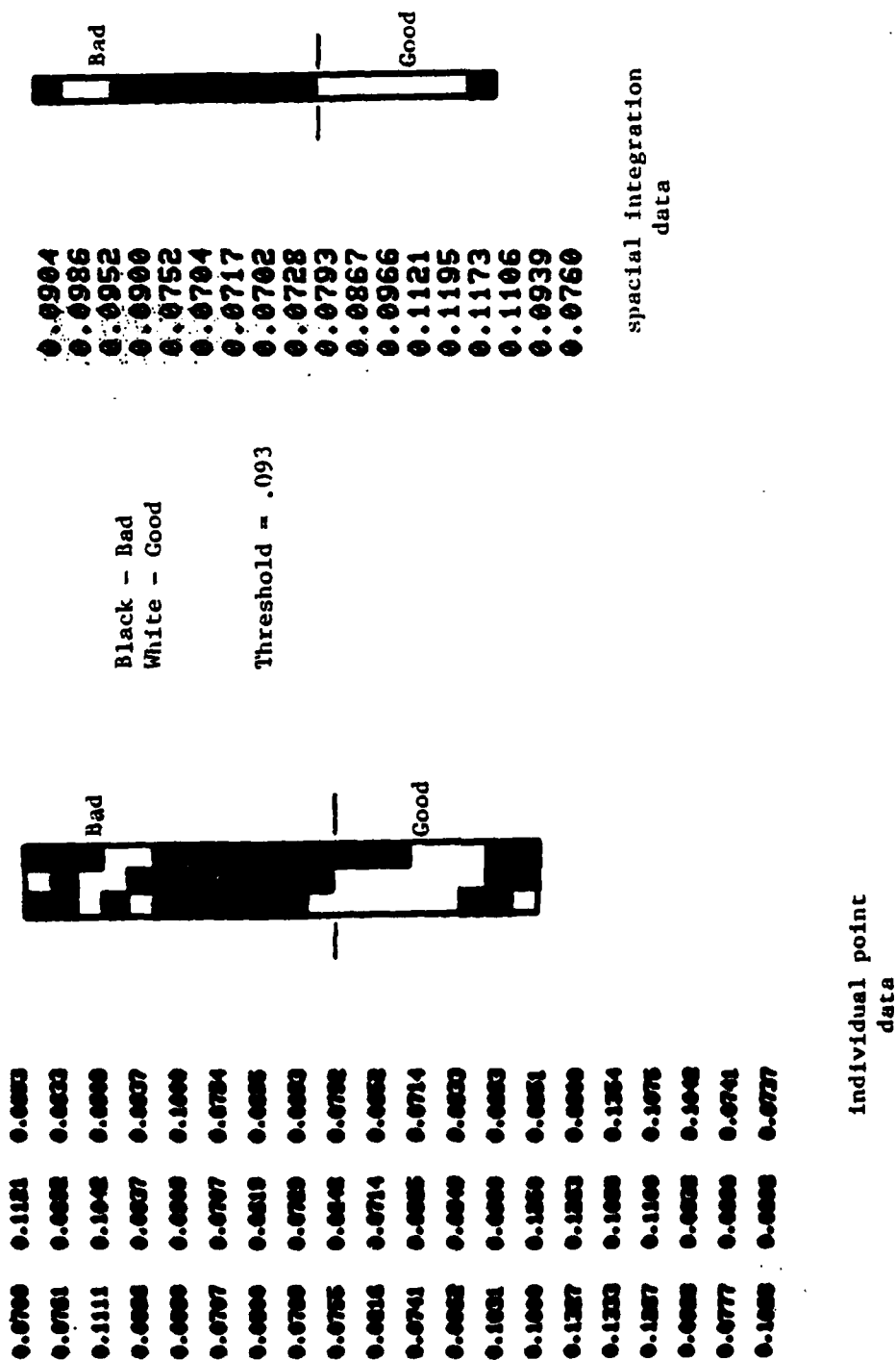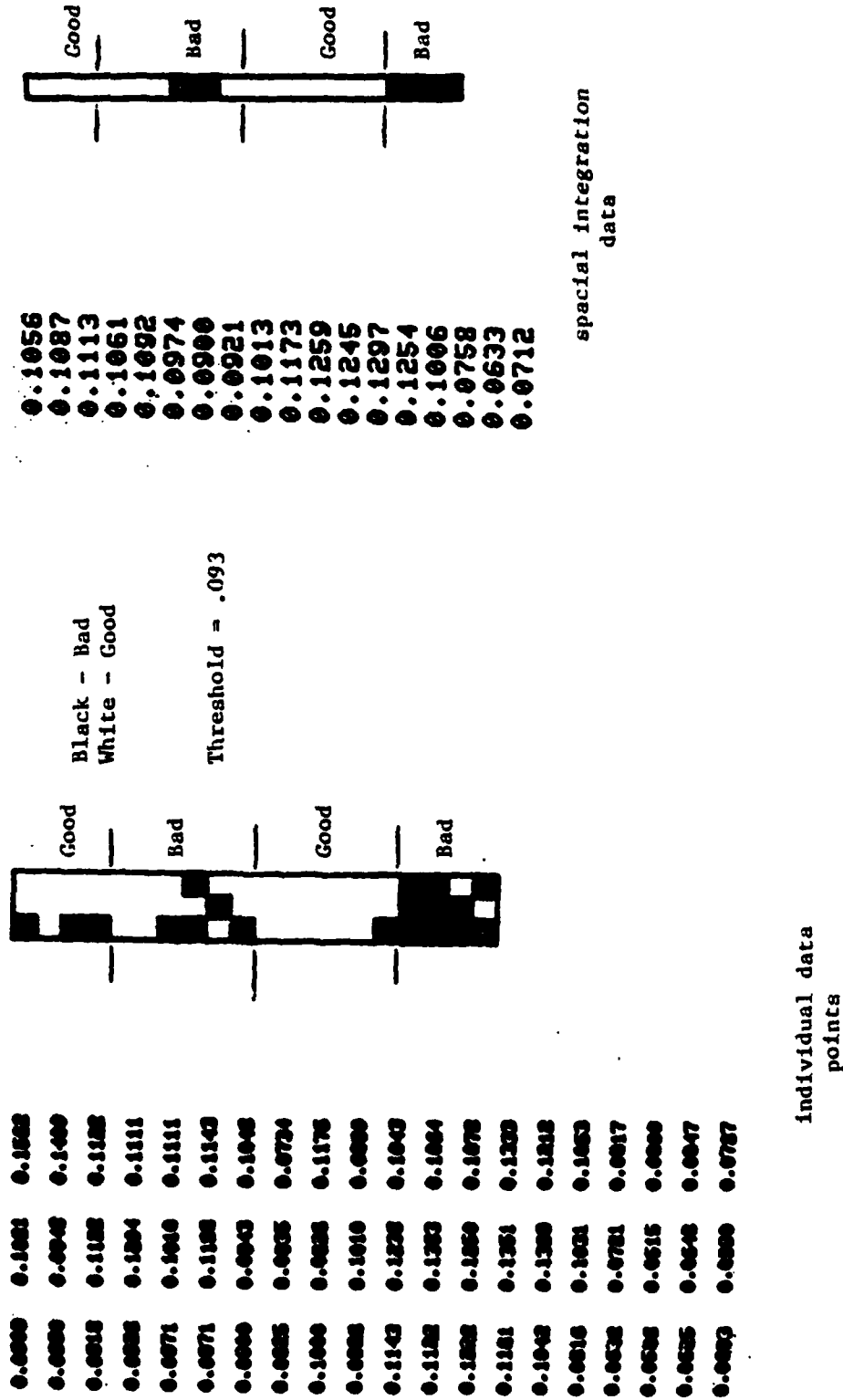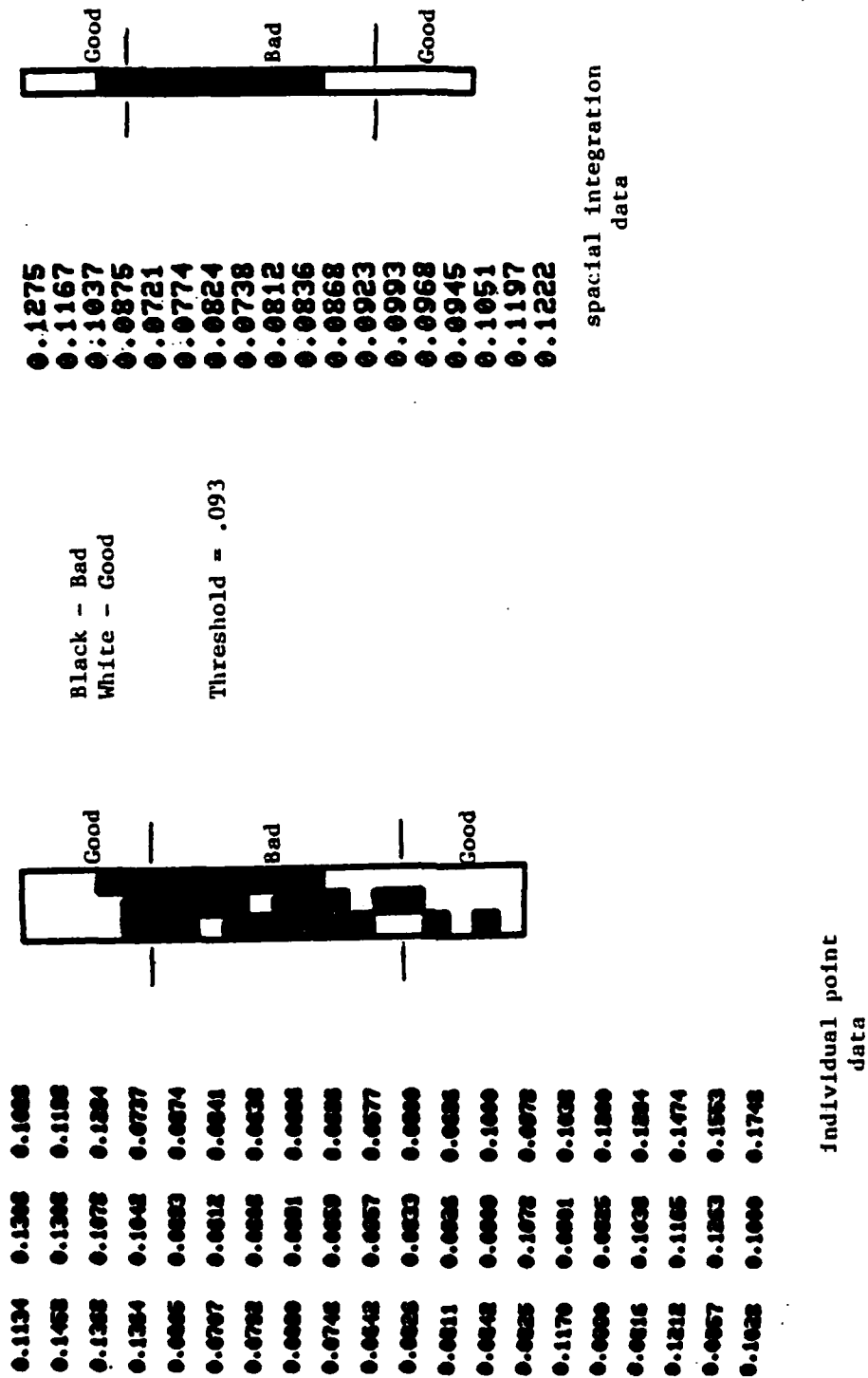
Figure 10.   Feature 5, Peak-to-Peak Ratio of Front Echo to Backwall Echo
(Specimen C, used to test threshold).

Figure 11.   Feature 6, Percent Frequency Content Below Mid-Frequency
(Specimen A, used to set threshold).

Good

Bad

Good

Bad

spacial integration
data

0.4086
0.3786
0.3482
0.3255
0.3179
0.3163
0.3141
0.3195
0.3263
0.3398
0.3616
0.4033
0.4293
0.4060
0.3587
0.3159
0.2770
0.2549

Black – Bad
White – Good

Threshold = .32

Good

Bad

Good

Bad

Individual point
data

Figure 12. Feature 6, Percent Frequency Content Below Mid-Frequency (Specimen B, used to test threshold).

33

Figure 13. Feature 6, Percent Frequency Content Below Mid-Frequency (Specimen C, used to test threshold).

Bad

Good

spacial integration
data

0.5601
0.5264
0.5135
0.5070
0.5178
0.5315
0.5461
0.5572
0.5474
0.5302
0.5319
0.5216
0.5027
0.4939
0.4799
0.4679
0.4649
0.4816

Black — Good
White — Bad

Threshold = .5

Bad

Good

individual point
data

Figure 14. Feature 7, Percent Frequency Content Above Mid-Frequency (Specimen A, used to set threshold).

Good

Bad

Good

Bad

spacial integration data

0.4517
0.4724
0.5084
0.5295
0.5402
0.5390
0.5347
0.5397
0.5329
0.5187
0.4984
0.4663
0.4508
0.4706
0.5150
0.5563
0.5811
0.6034

Black – Good
White – Bad

Threshold = .5

Good

Bad

Good

Bad

Individual point data

Figure 15. Feature 7, Percent Frequency Content Above Mid-Frequency (Specimen B, used to test threshold).

Good

Bad

Good

spacial integration
data

0.4864
0.4661
0.4726
0.4992
0.5233
0.5310
0.5475
0.5575
0.5654
0.5634
0.5541
0.5512
0.5455
0.5452
0.5296
0.4924
0.4661
0.4657

Black — Good
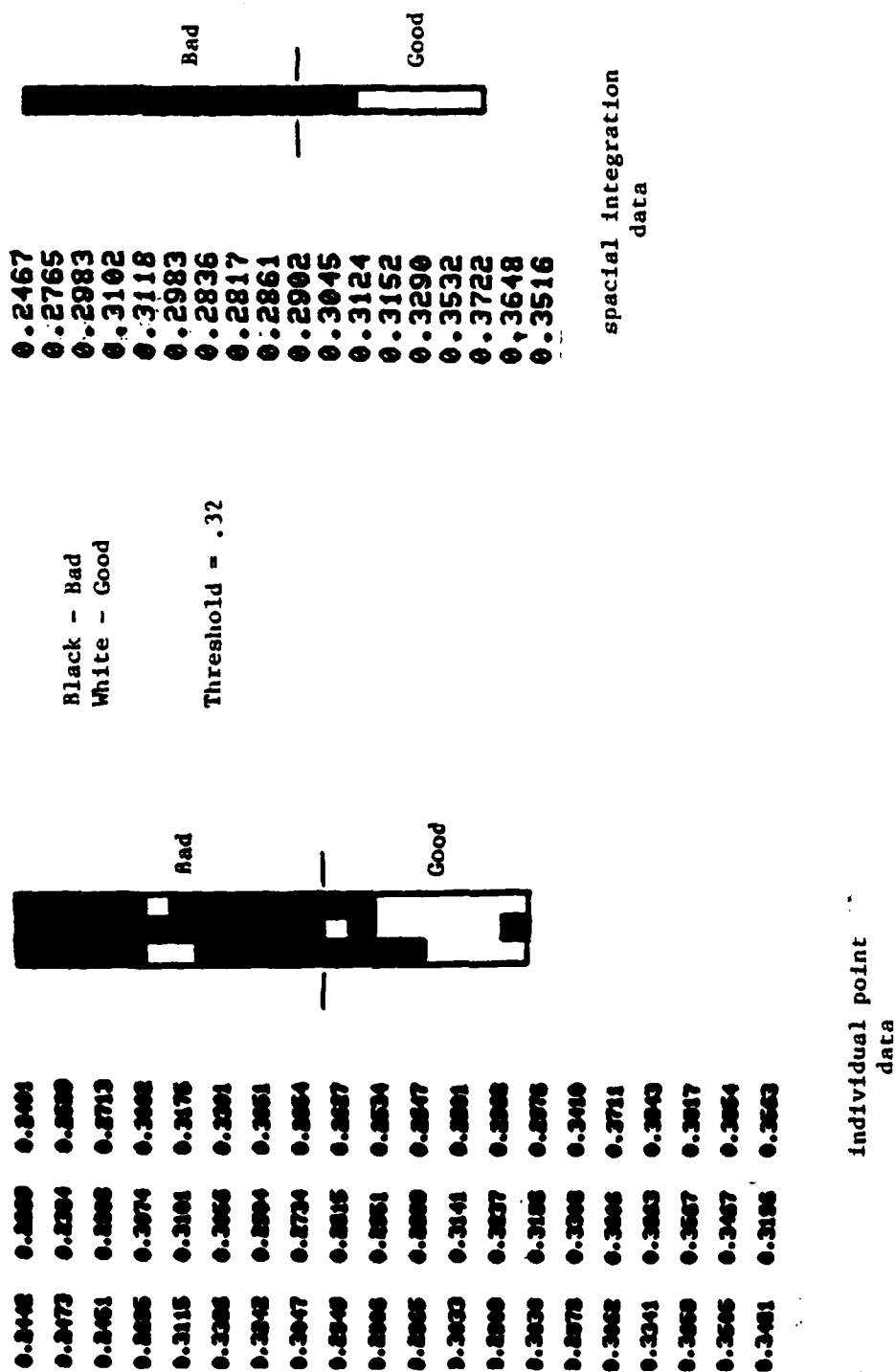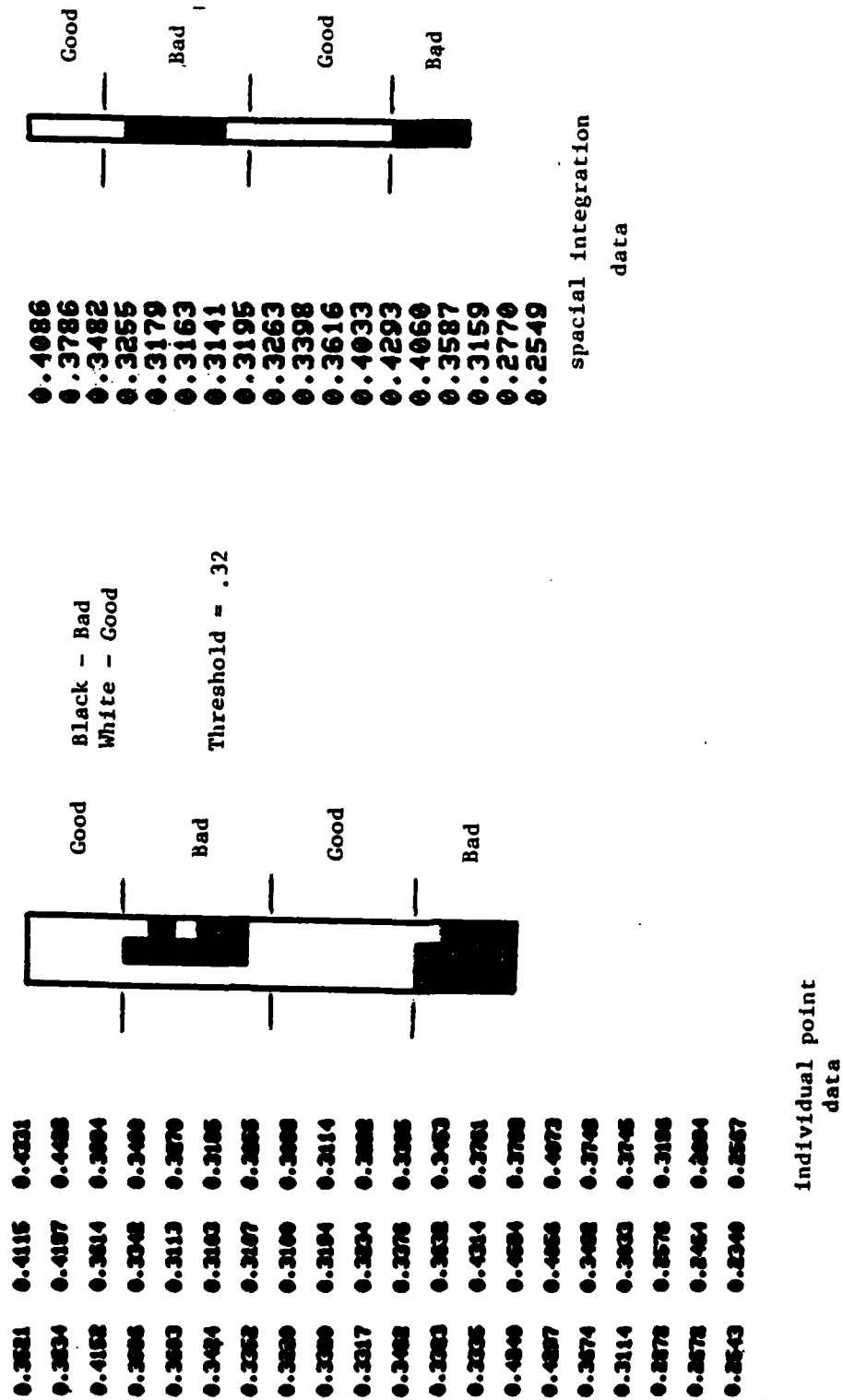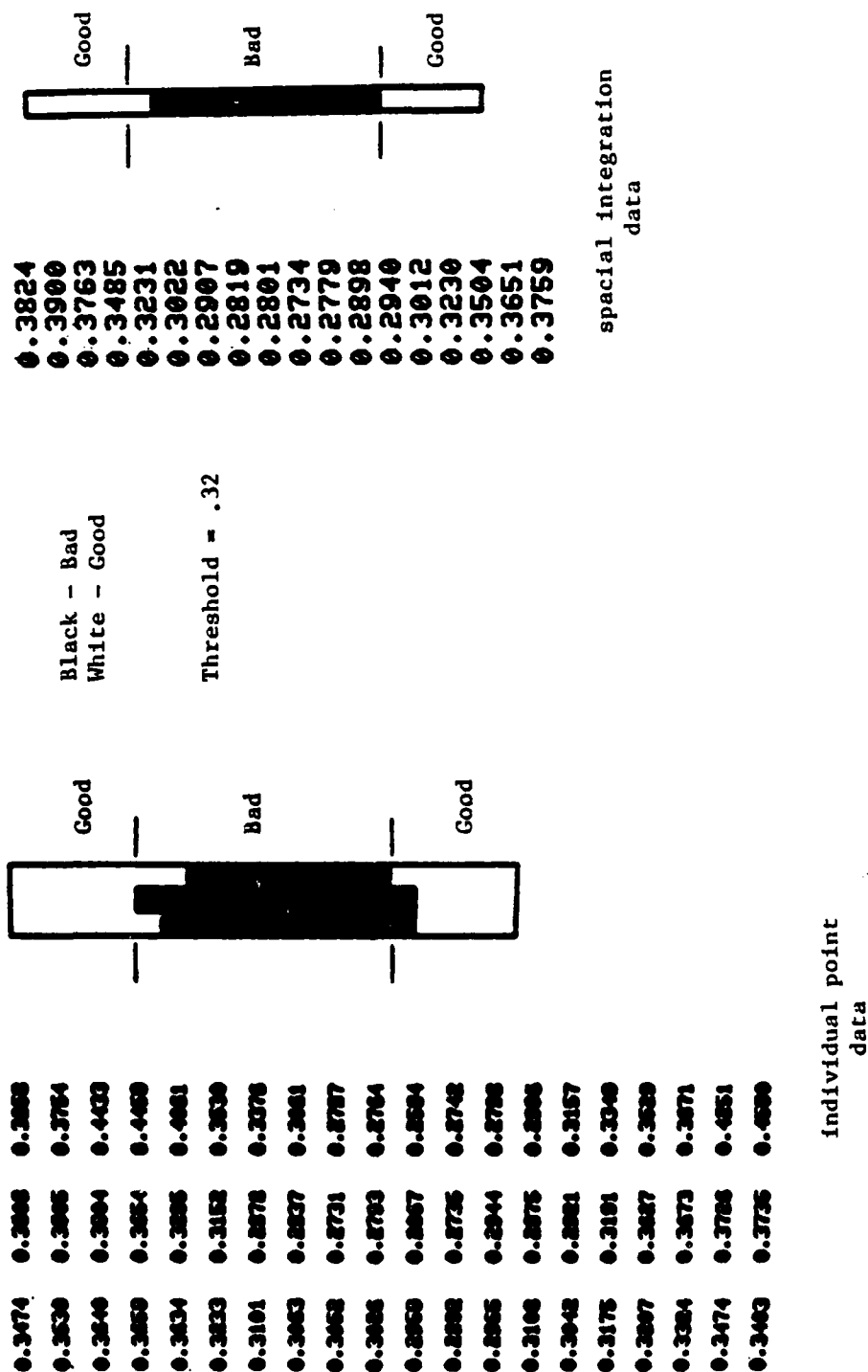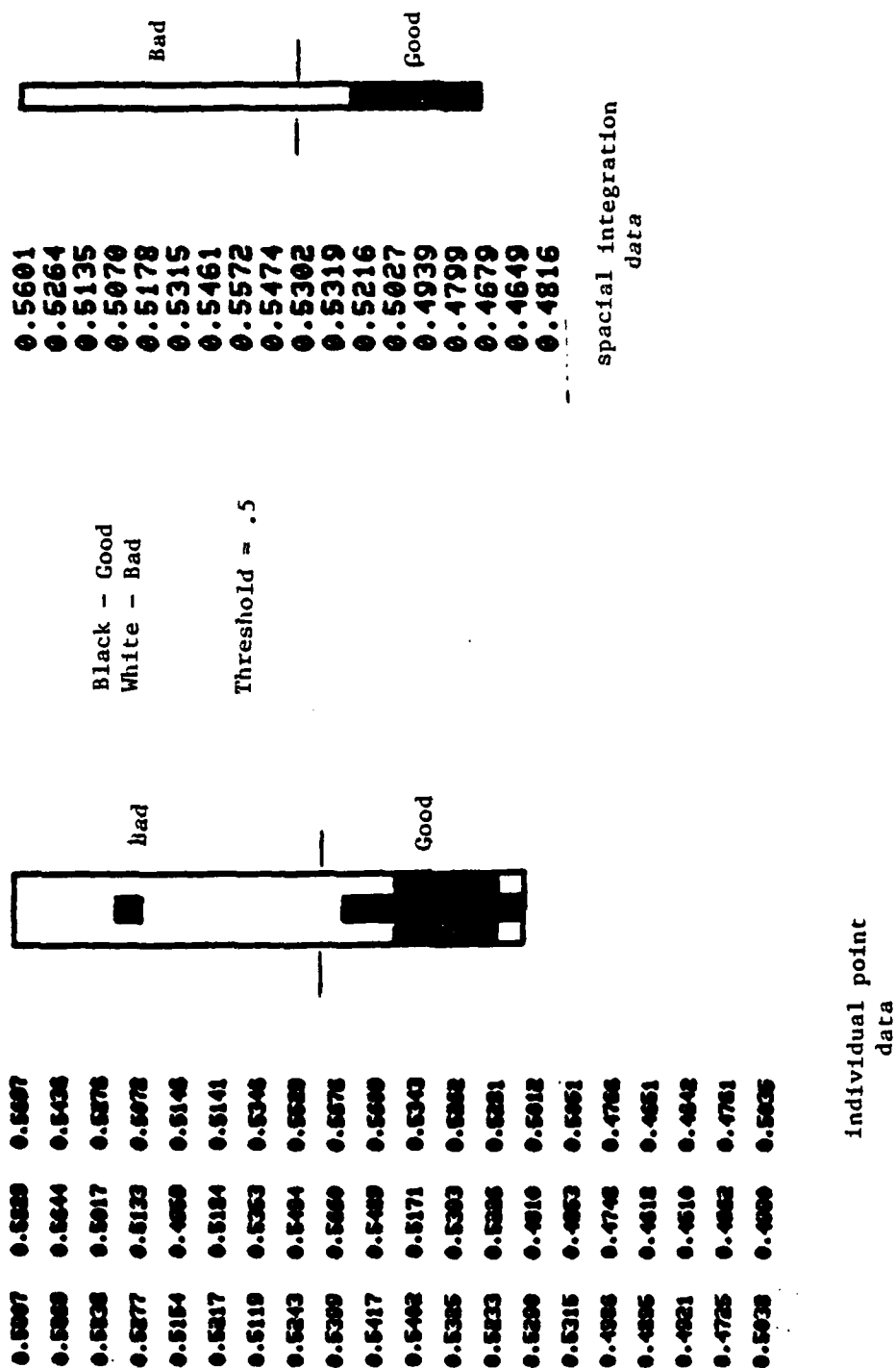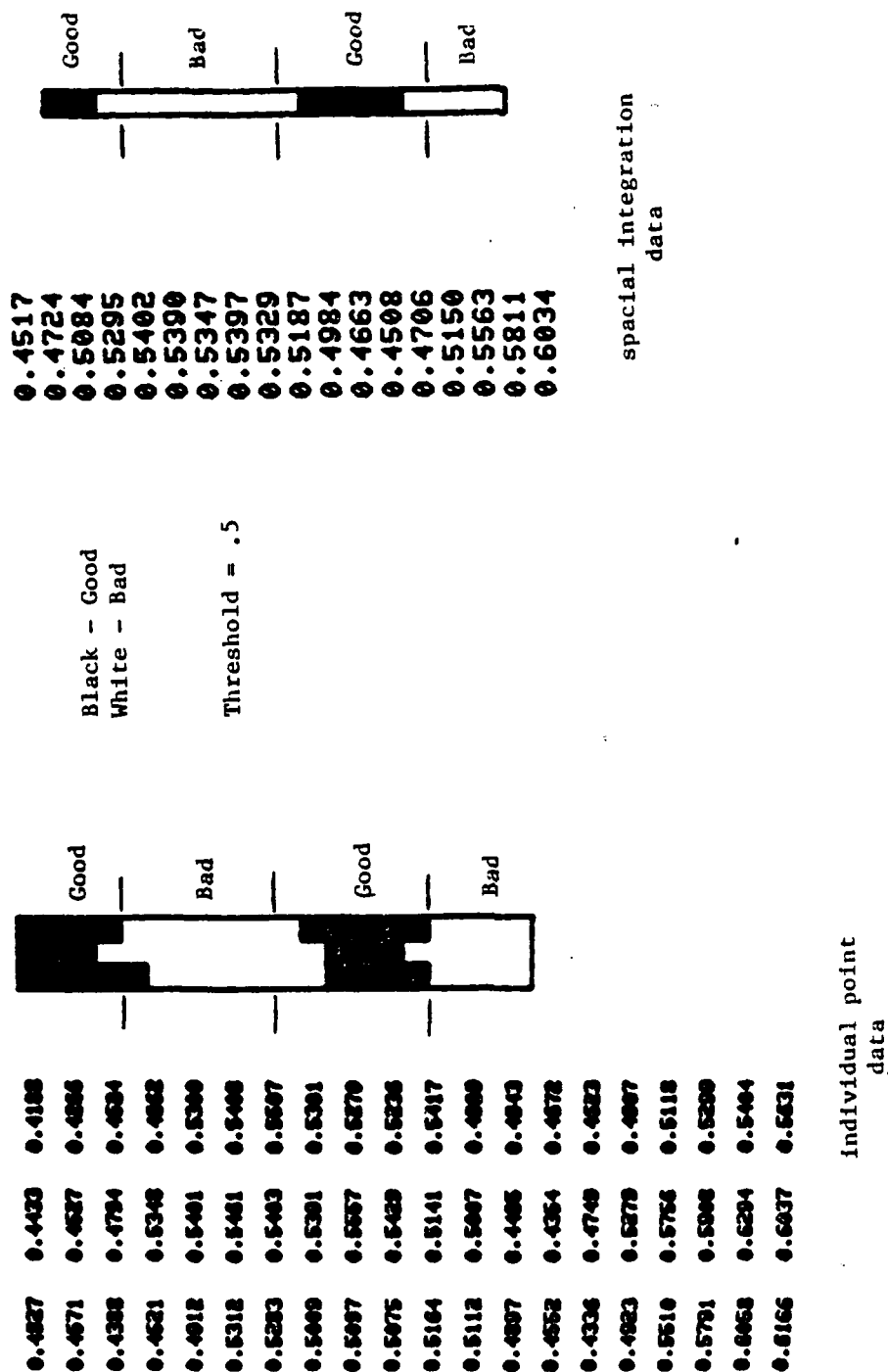White — Bad

Threshold = .5

Good

Bad

Good

individual point
data
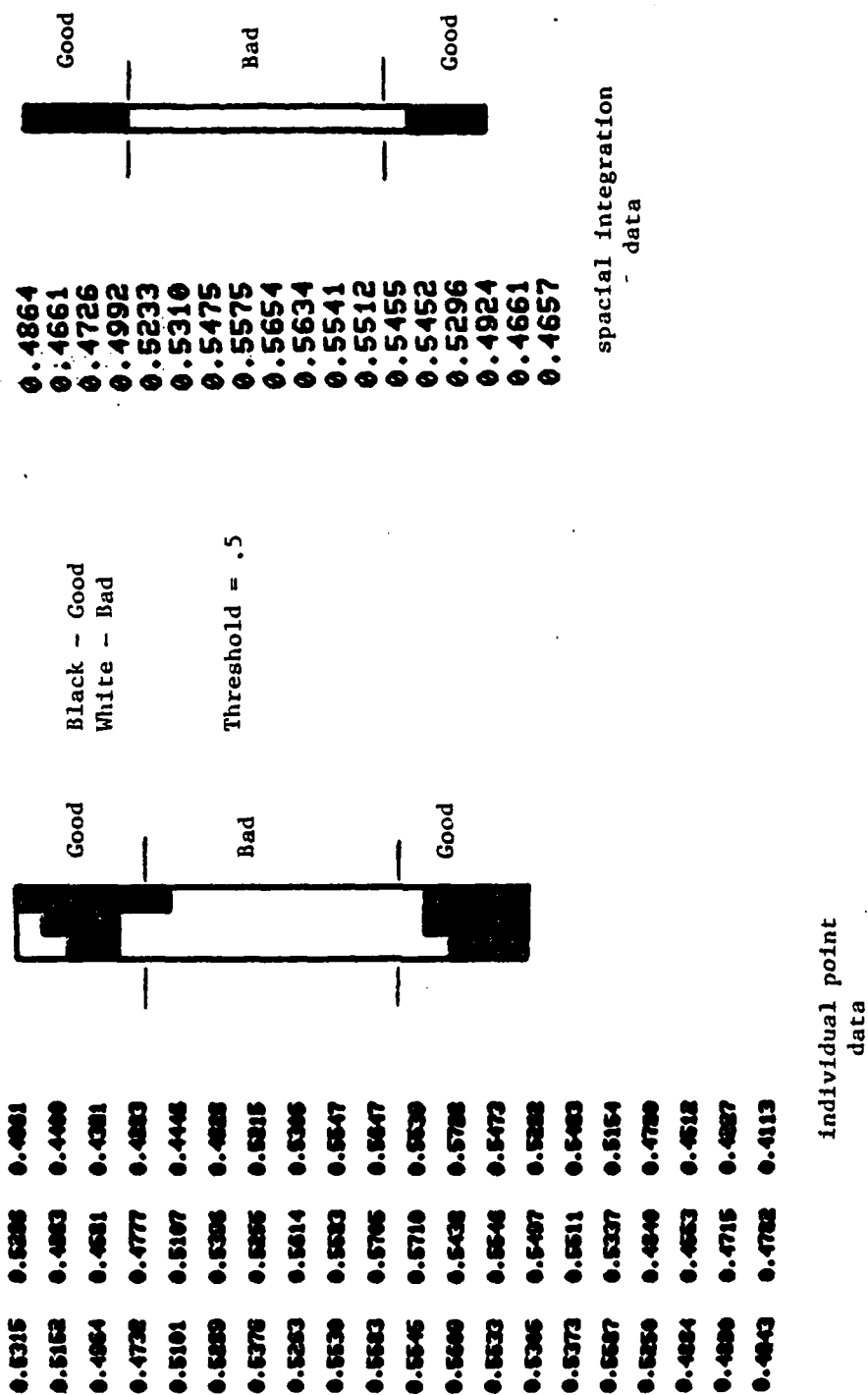
Figure 16. Feature 7, Percent Frequency Content Above Mid-Frequency (Specimen C, used to test threshold).
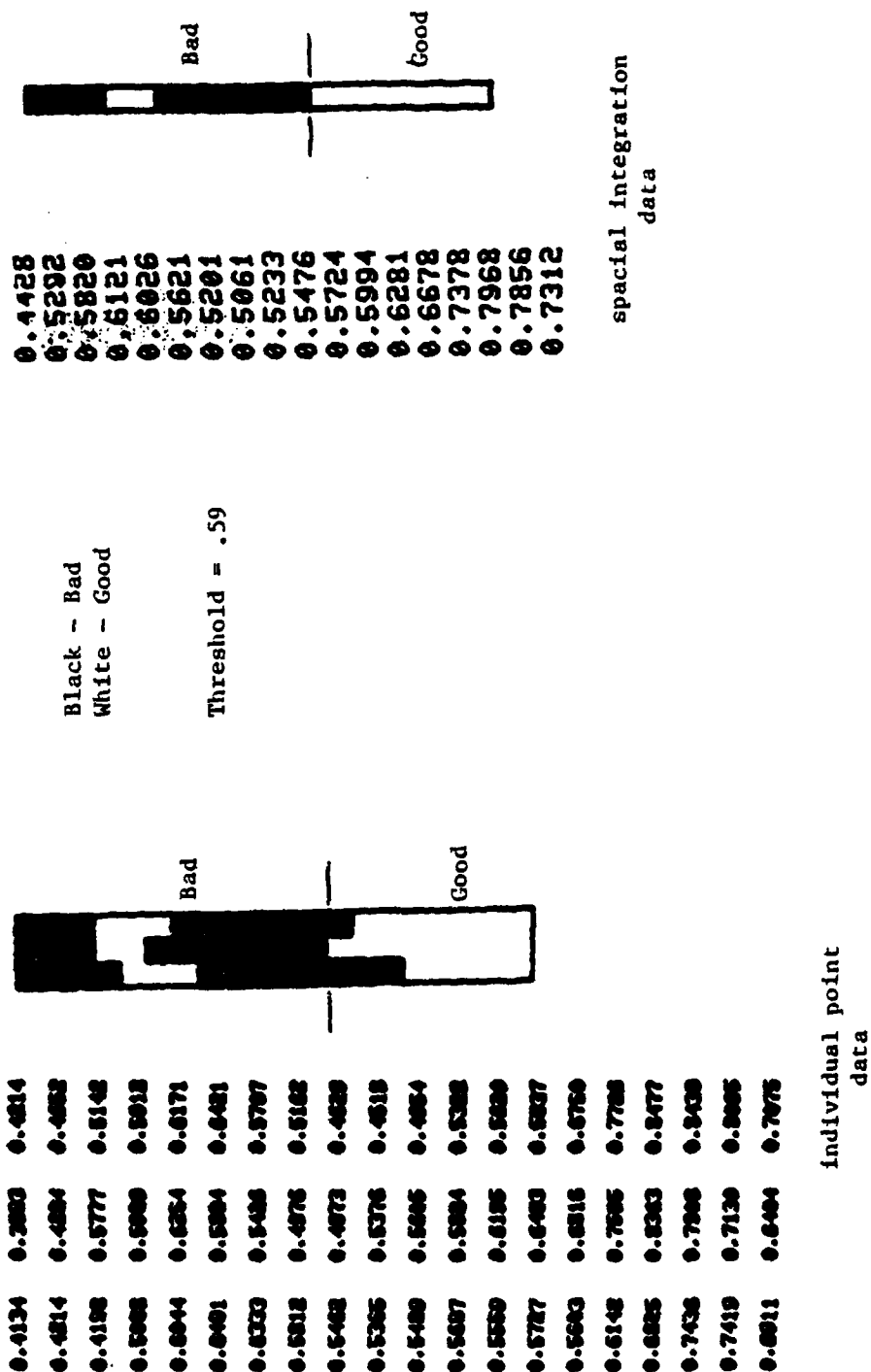
Figure 17. Feature 8, Ratio of Feature 6 to Feature 7 (Specimen A, used to set threshold).

Good
Bad
Good
Bad

spacial integration
data

0.9072
0.8073
0.6918
0.6176
0.5891
0.5871
0.5880
0.5928
0.6131
0.6558
0.7288
0.8716
0.9564
0.8686
0.7032
0.5727
0.4802
0.4247

Black – Bad
White – Good

Threshold = .59

Good
Bad
Good
Bad

individual point
data
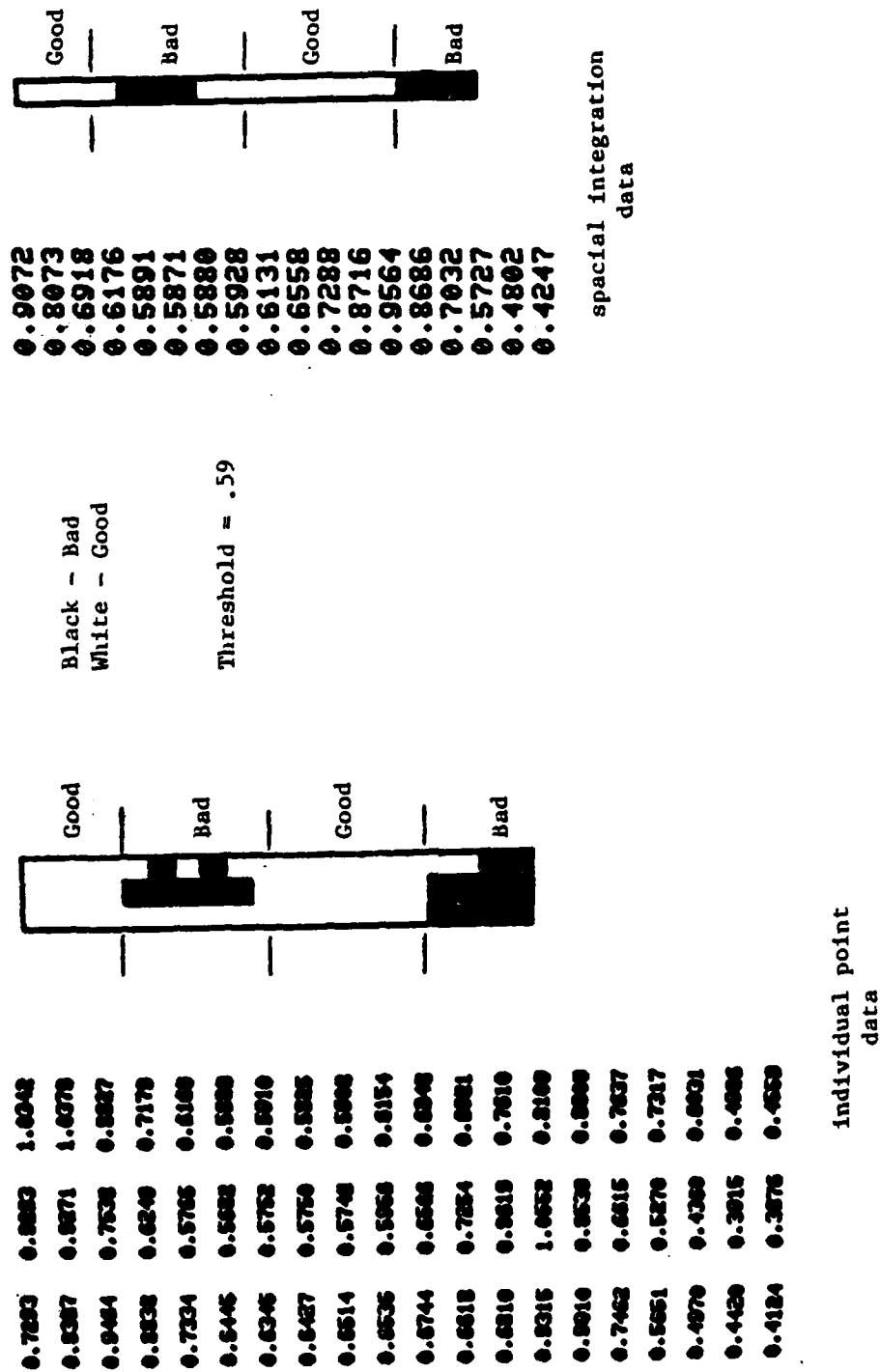
Figure 18.   Feature 8, Ratio of Feature 6 to Feature 7
(Specimen B, used to test threshold).

Good

Bad

Good

spacial integration
data

0.7896
0.8400
0.8014
0.7041
0.6203
0.5699
0.5319
0.5059
0.4955
0.4865
0.5018
0.5259
0.5392
0.5529
0.6124
0.7156
0.7857
0.8114

Black – Bad
White – Good

Threshold = .59

Good

Bad

Good

individual point
data
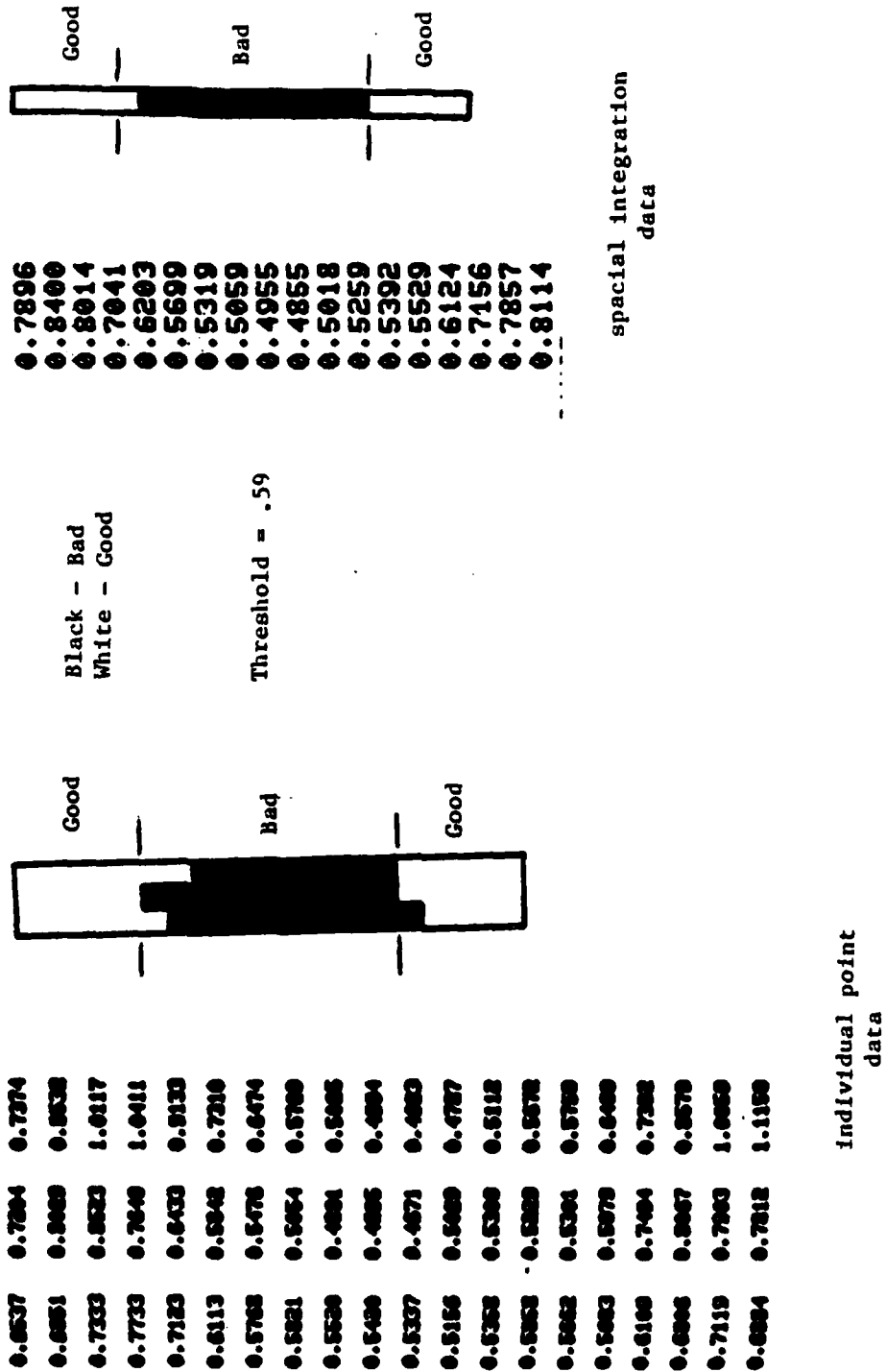
Figure 19. Feature 8, Ratio of Feature 6 to Feature 7 (Specimen C, used to test threshold).

DISTRIBUTION LIST

NAVAIRENGCEN
1114 (2)
1115
92A1C
92A3 (20)
92713
92A4
9011
91B1

NAVAIRPROPCEN PE43
AFML/LLP
AMMRC DRXMR-MQ
NAVSHIP R&D CENTER 2803

NAVAIRSYSCOM
AIR-00D4 (2)
AIR-340E (3)
AIR-552B
AIR-551132A
AIR-4114 (2)
AIR-5523 (2)
AIR-5203 (2)

NAVAIRDEVCEN 60633 (2)

DTIC (12)

REVISION LIST

REVISION	PAGES AFFECTED	DATE OF REVISION